

## Radiolarian faunal provinces in surface sediments of the Greenland, Iceland and Norwegian (GIN) Seas

K.R. Bjørklund<sup>a,\*</sup>, G. Cortese<sup>a,b</sup>, N. Swanberg<sup>c</sup>, H.J. Schrader<sup>d</sup>

<sup>a</sup> Paleontological Museum, University of Oslo, Sars gate 1, 0562 Oslo 5, Norway

<sup>b</sup> Earth Sciences Department, University of Florence, Via La Pira 4, 50129 Florence, Italy

<sup>c</sup> Royal Swedish Academy of Sciences, Lilla Frescativägen 4, S-104 05 Stockholm, Sweden

<sup>d</sup> Department of Geology, University of Bergen, Allégaten 41, N 5007 Bergen, Norway

Received 20 July 1997; accepted 8 April 1998

### Abstract

The overall abundance and species composition of the polycystine and phaeodarian radiolaria have been determined in 63 surface sediment samples from the GIN Seas. These results are compared to chemical and physical properties of the overlying water masses. There are three abundance maxima in the distribution of radiolarian skeletal debris preserved in these surface sediments, centered on the Iceland Plateau, southern Norwegian Basin and northern Norwegian Basin. The most commonly encountered species were: (a) Spumellarida —*Actinomma boreale*, *A. leptoderma*, *Larcospira minor*, and *Phorticium clevei*, (b) Nassellarida —*Amphimelissa setosa*, *Artobotrys boreale*, *Lithomelissa setosa*, *Lithocampe platycephala*, *Pseudodictyophimus gracilipes*, *Cycladophora davisiana*, and *Lithomitra lineata*. Based on factor analysis of the core-top assemblages, the radiolarian species were grouped into three associations: Factor 1 —a polar- and arctic water association dominated by *Amphimelissa setosa* (varimax factor score 5.269), high factor component values are found in the Iceland Plateau area and in a wedge just north of the Iceland–Faeroe Ridge; Factor 2 —an Atlantic water association dominated by *Pseudodictyophimus gracilipes* (3.247), *Lithomelissa setosa* (2.731), and *Actinomma boreale* (1.851), high factor component values are found in the eastern part of the Norwegian Sea, particularly in the area under the influence of the Norwegian Current; and Factor 3 —an Atlantic and arctic water mixed association dominated by *Lithocampe platycephala* (3.251), *Lithomelissa setosa* (–2.176), *Actinomma leptoderma* (1.994) and *Artobotrys boreale* (1.504), high factor component values are found immediately to the east of the Iceland Plateau in correspondence to the deepest part of the Norwegian Basin. The correlation coefficients obtained between seasonal sea surface temperature and Factors 1 ( $R^2 = 0.835$ ), and 2 ( $R^2 = 0.891$ ) show a good fit, whilst for Factor 3 there was a less marked ( $R^2 = 0.497$ ), but still significant at the 5% confidence level, correlation for fifth-degree polynomial regression functions. The factors correlated better with the summer than the winter sea surface temperatures. However, at 20, 50, 100 and 200 m depth, the correlation became increasingly better, particularly so for the winter situation. The highest species richness for polycystine radiolarians (>28 species) was found in the warm Atlantic domain, the lowest (<24 species) was found in the colder arctic and polar domains, whilst an area approximating the position of the Arctic front had between 24 and 28 species. © 1998 Elsevier Science B.V. All rights reserved.

**Keywords:** radiolaria; Recent; Norwegian Sea; Iceland Sea; paleotemperature; factor analysis

\* Corresponding author. Tel.: +47 2285-1669; E-mail: kjell.bjorklund@toyen.uio.no

## 1. Introduction

The region occupied by the Greenland, Iceland, and Norwegian (GIN) Seas (Fig. 1) is liable to major changes in oceanographic conditions, and thus the fossil record in the sediments of the region offers a particularly sensitive indicator of palaeoceanographic changes. Kellogg (1976) demonstrated that the position of the polar front, now in the western GIN Seas at above 70°N, was located in the North Atlantic at about 45°N latitude during the last glacial maximum. The hydrographical setting (Fig. 2a–c) with cold, low-salinity arctic water masses in the west and warm, high salinity Atlantic water masses in the east, changed through the latest glacial–interglacial cycle (Koç-Karpuz and Schrader, 1990; Koç et al., 1993, 1996). The various modern water masses can be recognized not only by their hydrographical parameters, but also by their micro-, zoo-, and phytoplankton assemblages. The study of these assemblages can provide information, in space and time, on surface and subsurface water temperatures, water mass boundaries, oceanographic fronts and surface currents, Fig. 3.

The palaeontological record of the GIN Seas has been studied in detail by several authors in an attempt to reconstruct the sequence of oceanographical developments in the region during the last 18 Ka. Most such reconstructions are based on distributions of planktonic foraminifera (Kellogg, 1976, 1984; Johannessen et al., 1994). Unfortunately, the species richness of planktic foraminifera in the high latitudes of the GIN Seas is low (ca. 9 species, Kellogg, 1976) compared to that of tropical areas (ca. 30 species, Tolderlund and Bé, 1971; Bé and Hutson, 1977). The planktic foraminiferan assemblage of the GIN Seas is, according to Kellogg (1976), almost monospecific: *Neogloboquadrina pachyderma* (dextral) represents 95% or more of the assemblage, while *N. pachyderma* (sinistral) and four additional species are common: *Globigerina bulloides*, *G. quinqueloba*, *Globorotalia inflata* and *Globigerinita glutinata*. An additional four species are listed as rare in the appendix (microfiche) of Kellogg (1975). The low species richness of planktonic foraminifers in the north Atlantic and in the GIN Seas reduces the reliability of planktic foraminifera transfer function palaeo-temperature estimates (Le and Shackleton, 1994). The high diver-

sity of both diatoms and radiolarians in the study area potentially allows a more reliable use of this technique. The data presented herein have been used to develop a palaeo-temperature transfer function for the last ca. 13 500 years B.P. in the southeastern Norwegian Basin (Dolven, 1998).

Pflaumann et al. (1996) present a new method of temperature estimation (SIMMAX) which can be used to link faunal assemblages and sea surface temperature measurements. SIMMAX, according to Pflaumann et al. (1996), is a “... modern analog technique (Hutson, 1980), directly measures the difference between the faunal composition of a subject sample with a subset of best analogs of a modern assemblage dataset selected by a similarity or dissimilarity index and estimates a temperature as the average or weighted average of the ‘measured’ temperatures at the stations with the best analogs”. There are advantages and disadvantages in using SIMMAX (Pflaumann et al., 1996) or CABFAC (Klovan and Imbrie, 1971). The reader is referred to Pflaumann et al. (1996) for a more thorough discussion of the topic.

In one study in the area ca. 70 diatom species were used to define diatom associations from the surface sediments of the north Atlantic and the GIN Seas, and to extract palaeo temperature estimates during the last 14 Ka (Koç-Karpuz and Schrader, 1990; Koç et al., 1993, 1996).

Radiolarian fossils are also of potential value in palaeoclimatic reconstructions, but so far few palaeoclimatic interpretations and reconstructions in the GIN Seas have been based on radiolarian distributions (see Jansen and Bjørklund, 1985, and more recently Molina-Cruz and Bernal-Ramirez, 1996). The polycystine radiolarian assemblages of the GIN Seas have only been studied extensively from a taxonomical point of view (Cleve, 1899, 1900; Jørgensen, 1900, 1905; Schröder, 1909, 1914). Bjørklund (1976) presented photographs of many of the species described by Jørgensen (1900, 1905), based on Jørgensen’s slides. The fauna found in Recent sediments is composed of about 70 species (Petruševskaya and Bjørklund, 1974). Samtleben et al. (1995) reported 50 species from the sediment and 60 from the water column, making radiolarians the most species-rich micro-zooplankton group found in both the plankton and sediments in the GIN Seas. We have identified 75 species in the sediments (Appendixes A

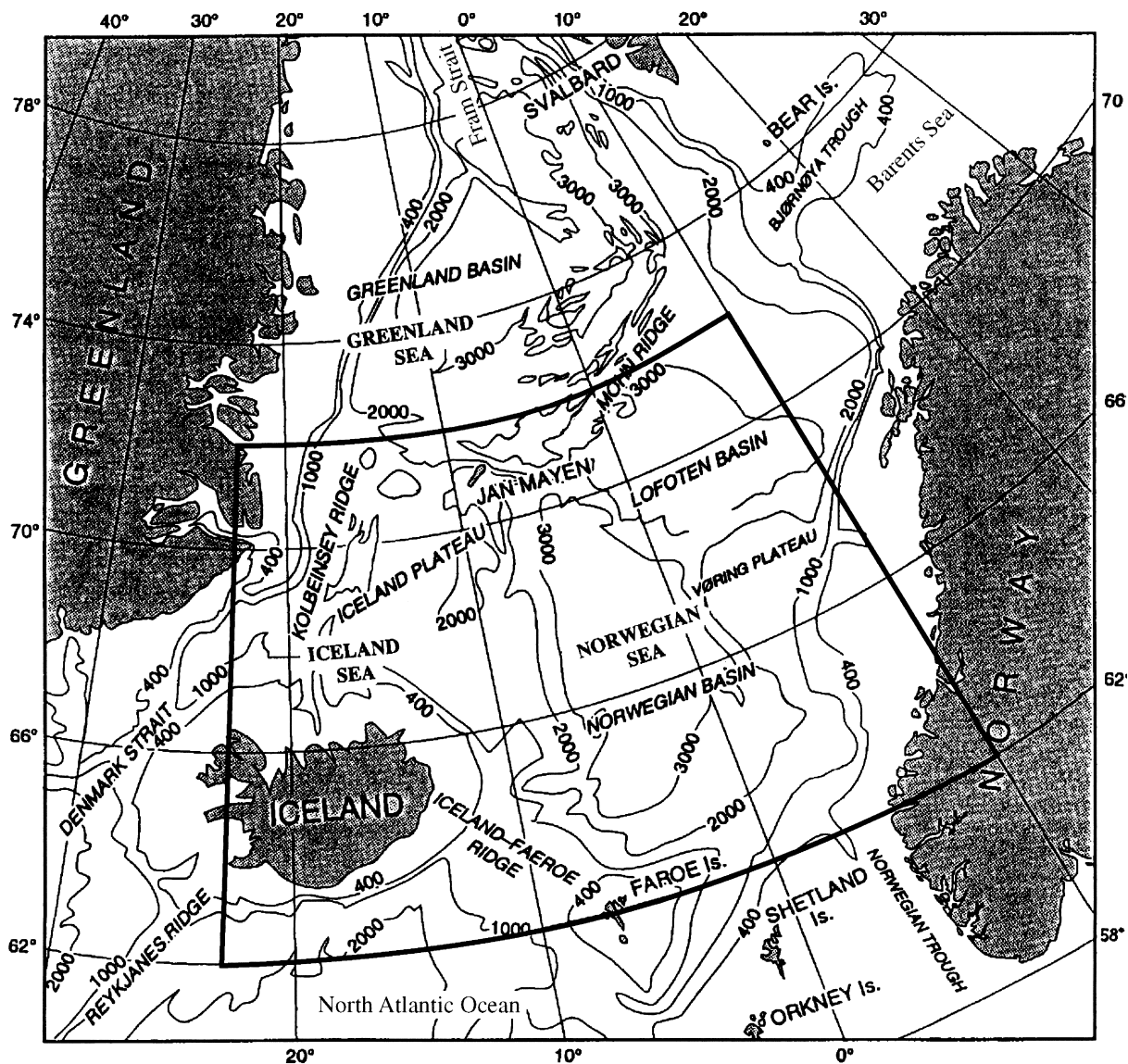


Fig. 1. Map of the Greenland, Iceland and Norwegian Sea (redrawn after Eldholm et al., 1990). The marked box shows the location of the study area.

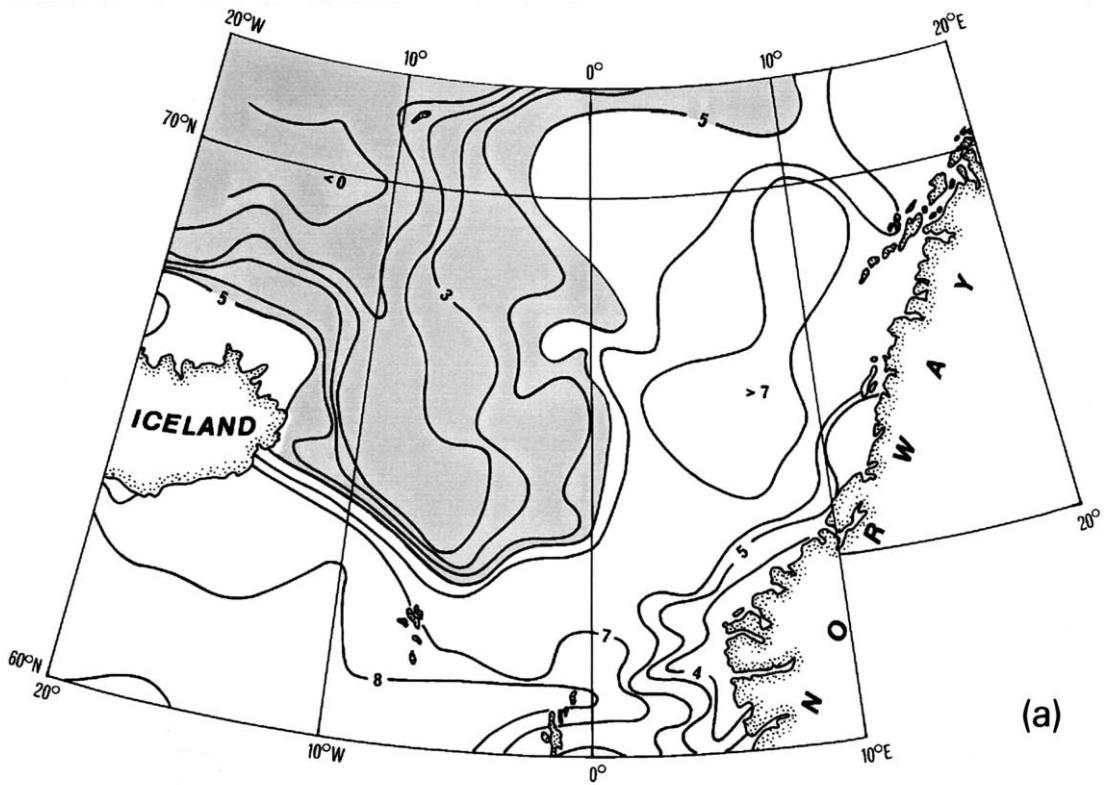
and B), however, only those that have been included in the CABFAC analysis are illustrated in this paper (Plates I and II).

## 2. Oceanographic setting and water masses

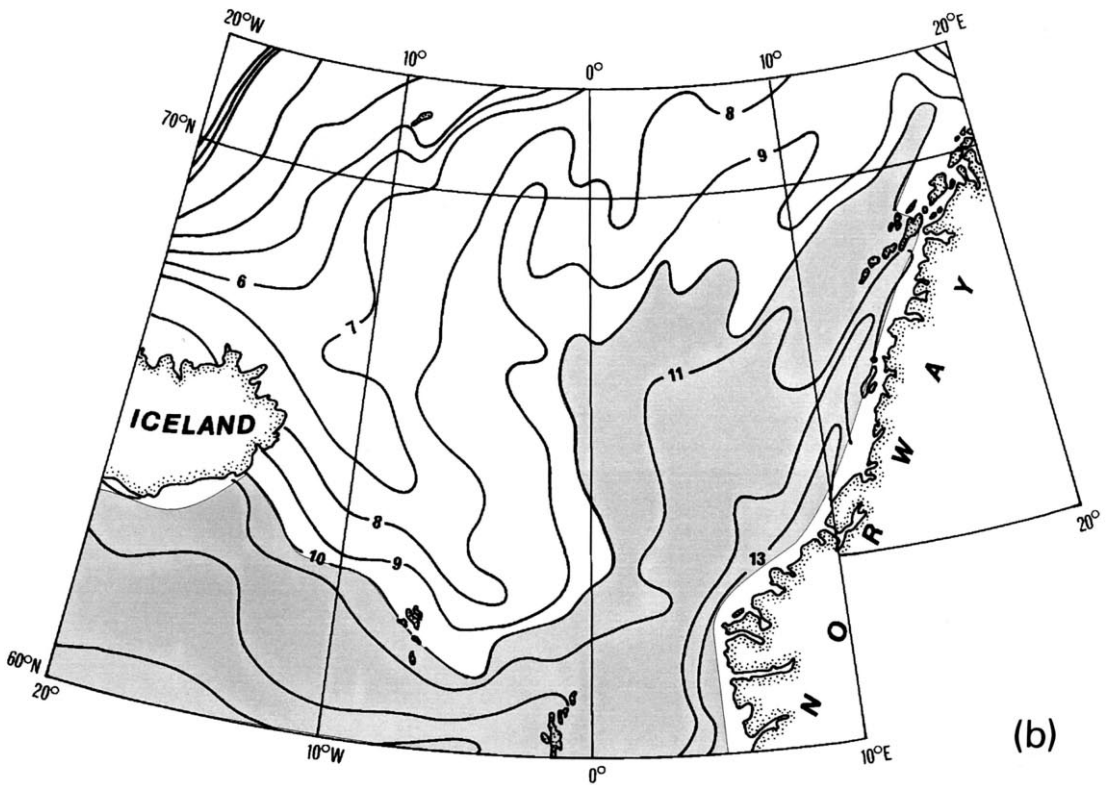
The GIN Seas are connected to the polar province through the Barents Sea and the Fram Strait, and to the North Atlantic Ocean over the Iceland–Faeroe

Ridge, Fig. 1. The formation of these gateways between the Atlantic and the Arctic Oceans led, during mid to late Neogene, to extensive changes in the palaeoceanography of the Atlantic Ocean, allowing exchange of cold waters between polar and subpolar deep-sea basins (Schäfer et al., 1995).

The Greenland and Iceland Seas are now areas of intensive formation of deep-water. Water mass definitions are given in Table 1 from Swift and



(a)



(b)

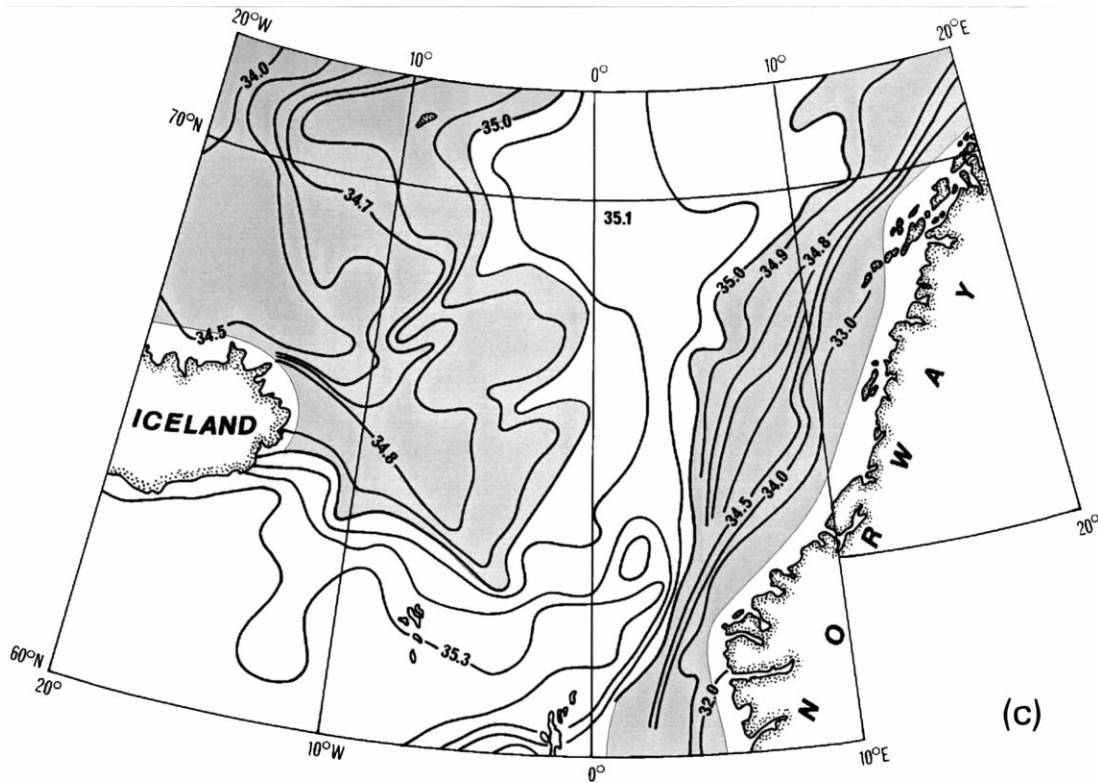


Fig. 2 (continued). (c) Salinity in the surface waters of the GIN Sea (redrawn from Dietrich, 1969), 0.1 psu isohales. Areas where salinity is lower than 35 psu are shaded.

Aagaard (1981), who also give a detailed description of the hydrography of the GIN Seas.

Two surface current systems, the warm North Atlantic Drift also referred to as the Norwegian Current and the cold East Greenland Current (EGC), have gyres that merge in the GIN Seas, Fig. 3. Due to cooling and mixing of the Atlantic Water (AW) with other water masses in the Greenland and Iceland Seas, cascades of Greenland Sea Deep Water (GSDW) and Norwegian Sea Deep Water (NSDW) are formed. AW is the primary source of GSDW (Swift and Aagaard, 1981). AW and Arctic Sea Water (ASW) appear not to mix before cooling, because they are separated by the Arctic Front, Fig. 3. As the Norwegian Sea and half of the Iceland and Green-

land Seas remain ice-free during winter, Swift and Aagaard (1981) concluded that the contribution of AW had to predominate, otherwise the low density Polar Water (PW) could rapidly stratify the surface layer and permit winter ice formation.

The close juxtaposition of warm and cold water masses results in the formation of distinct oceanographic fronts. Between these two main water masses, mixed Arctic surface water is formed in two large gyres (the East Iceland Current and the westward branching of the Norwegian Current, Fig. 3). The inflow of warm North Atlantic water, which is the main conduit for heat transport from the low latitude Atlantic into the high northern seas, takes place across the Iceland/Faeroe Ridge, and at

Fig. 2. (a) Winter surface water temperature in the GIN Sea (redrawn from Dietrich, 1969), 1°C isotherms. Areas where temperature is lower than 5°C are shaded. (b) Summer surface water temperature in the GIN Sea (redrawn from Dietrich, 1969), 1°C isotherms. Areas where temperature is higher than 10°C are shaded.

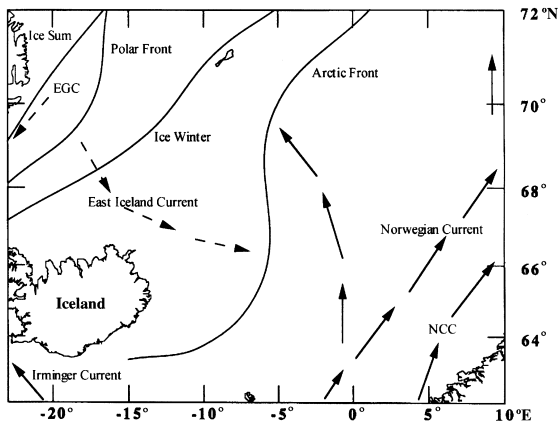


Fig. 3. Warm (arrows) and cold (dashed arrows) surface currents, Polar and Arctic fronts (redrawn after Samtleben et al., 1995) and summer and winter position of the ice-edge (Schäfer et al., 1995). The surface currents pattern has been simplified by removing the secondary branches of the main currents.

a smaller scale through the Denmark Strait (Irminger Current).

For this study, the surface waters in the area have been characterized, according to Swift and Aagaard (1981), in three major water masses (Table 1):

- AW (the Norwegian Current with its Atlantic Water) with salinities above 34.9 practical salinity units (psu) and temperatures above 3°C;
- PW (the East Greenland Current with its Polar Water) with salinities below 34.4 psu and temperatures below 0°C;
- ASW (Arctic Sea Water) with salinities between 34.4 and 34.9 psu and winter temperatures below 0°C.

According to Hopkins (1988) the Arctic Front (defined by the 35 psu isohale and reaching a depth

of ca. 350 m) is a rather stable oceanographic feature both between seasons and years. However, mesoscale eddies, 30–40 km in diameter, are forming along the Arctic Front, but they are only surface and transient features reaching down to ca. 50 m (Niiler et al., 1992).

### 3. Materials and methods

Core-top samples from 229 stations were available to cover the southern GIN Seas. The radiolarian abundance was determined in all those stations (Fig. 4) within the mapping area.

Stations for detailed study were selected on the basis of the abundance of radiolarian remains and

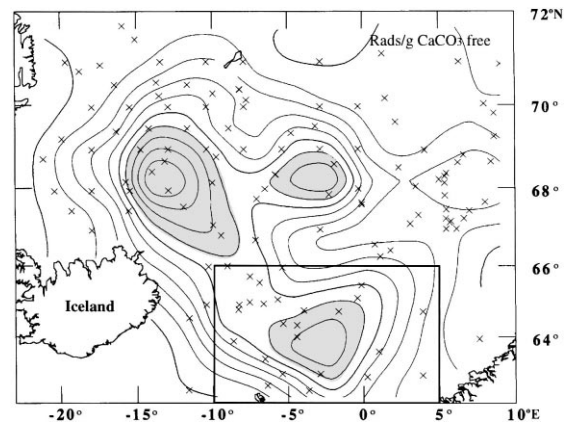


Fig. 4. Number of radiolarians per gram  $\text{CaCO}_3$  free sediment. Areas with more than 60 000 radiolarians per gram  $\text{CaCO}_3$  free sediment are shaded. Increment between isolines = 10 000; heavy line increment = 50 000. This map is based on analysis of 229 samples, from which 63 were selected for the main study. The box shows the location of the area plotted in Fig. 5.

Table 1  
Water mass definitions for the GIN Seas after Swift and Aagaard (1981)

Water mass name	Temperature (°C)	Salinity (psu)
Atlantic Water (AW)	>3	>34.9
Arctic Sea Water (ASW)	<0	34.4 to 34.9
Polar Water (PW)	<0	<34.4
Lower Arctic Intermediate Water (lower AIW)	0 to 3	>34.9
Upper Arctic Intermediate Water (upper AIW)	ca. 2	34.7 to 34.9
Polar Intermediate Water (PIW)	<0	34.4 to 34.7
Greenland Sea Deep Water (GSDW)	< -1	34.88 to 34.90
Norwegian Sea Deep Water (NSDW)	< -0.4	34.90 to 34.94

by the following criteria, as recommended by Imbrie and Kipp (1971):

- (a) The stations should have a reasonably even geographic distribution;
- (b) The sample set should underlie surface waters with a wide range of salinities and temperatures;
- (c) Core tops with dissolution should be avoided (we have also avoided stations with severe fragmentation);
- (d) Core tops with significant amounts of nonpelagic material should be avoided;
- (e) The core tops should contain only Recent radiolarians.

This led to a selection of 63 samples (Table 2).

Most of the core-top material used in this study was obtained from the topmost 1–2 cm of the Trigger weight (TW) cores from the core libraries at the Lamont-Doherty Earth Observatory, Columbia University (*R/V Vema* cruises 23, 27, 28, 29, and 30), and the Department of Oceanography, University of Washington (*USS Edisto* 1963 cruise). Some additional cores were made available to us from the Geological Institute, University of Bergen (*R/V Håkon Mosby* cruise 31).

The techniques used to separate the radiolarian skeletons from the sediment have been described earlier by Goll and Bjørklund (1974). The sieve size used was 45  $\mu\text{m}$ .

We counted, in arbitrarily selected fields of view, between 327 and 570 specimens (Appendix B) identified as far as possible to species level. During this counting we encountered a total of 75 species. The counting categories included Spumellarida indet. (not identified) and Nassellarida indet. These two groups are negligible in some areas, constituting less than 5% of the total fauna, while in other areas they can be quite significant; often mainly juveniles and fragmented larcoids. These two groups are included when calculating the species percent values.

The species that were treated statistically had to meet the following criteria, recommended by Imbrie and Kipp (1971): (1) the species had to occur as more than 2% of the total fauna in at least one station and (2) had to occur in at least 10 stations. After this selection was applied, 28 species remained for analysis.

Our goal was to correlate the GIN Seas radiolarian sediment species assemblages with modern overlying oceanographical parameters such as tem-

perature, salinity and nutrients concentration. There are several temperature datasets available from the GIN Seas (USNHO, 1958; USNOO, 1967; Dietrich, 1969; Kellogg, 1975; Levitus, 1982; ICES, 1996). In addition we had access to data for salinity (Dietrich, 1969), phosphate, nitrate, and nitrite (ICES, 1996). We finally used Dietrich (1969) temperatures, because this dataset gives a more accurate and realistic picture of the temperature and salinity distribution in the GIN Seas. An evaluation of the dataset best suited for our correlations will be given in Section 5.

The Imbrie and Kipp (1971) factor analysis method and the FORTRAN program CABFAC (Klovan and Imbrie, 1971) were used for the statistical treatment of the dataset.

The program Mercplot, developed by Tim Schrader for the POC (Predicting Ocean Climate) Program, Geological Institute, University of Bergen (Norway), was used to produce the contour maps. A Laplacian algorithm was used by the program to interpolate and draw contour lines. This algorithm was applied to a  $15 \times 15$  grid (coinciding with the study area), whose 225 elements were further subdivided in 8 grid boxes each, using cubic polynomial interpolation.

In this study we have included the Phaeodaria in our counts, because they occur in a significant amount in the GIN Seas surface sediments, a special phenomenon for these northern seas. When we are using the informal name radiolarians in this study, we include both Phaeodaria and Polycystina.

## 4. Results

### 4.1. Distribution of radiolarians in the surface sediments of the GIN Seas

The abundance of radiolarian skeletons in the surface sediments of the GIN Seas, on a carbonate-free basis, is shown in Fig. 4.

The program used to plot this figure displays and smooths three areas of high radiolarian concentrations, and interpolates the abundance data which have maxima that are actually higher than shown in Fig. 4. The high radiolarian abundance areas are located on the Iceland Plateau (peak value, 155 000 skeletons/g at station V27-47) and in both the southern (101 000 skeletons/g at station ED-87)

Table 2

Station list (Edisto, Vema and Haakon Mosby cruises) reporting, for each station, latitude, longitude, depth, carbonate content, number of radiolarians per gram CaCO<sub>3</sub> free sediment, number of radiolarians per gram bulk sediment, salinity (Dietrich, 1969), summer and winter surface temperatures from Dietrich (1969), Kellogg (1975) and Levitus (1982), respectively and ICES (1996) summer surface temperatures

Station	Latitude	Longitude	Depth (m)	CaCO <sub>3</sub> (%)	Rads/gr CaCO <sub>3</sub> free	Rads/gr bulk	Sal Die	ST Die	WT Die	ST Kel	WT Kel	ST Lev	WT Lev	ST ICE
ED-14	69.00.0 N	05.00.0 W	3340	49.3	56600	28700	34.96	8.4	3.5	8.0	2.4	6.8	3.2	4.2
ED-15	69.00.0 N	07.30.0 W	2560	18.3	3300	2700	34.82	7.7	2.0	7.0	1.3	5.8	2.2	2.9
ED-17	69.00.0 N	10.00.0 W	2200	53.7	66500	30800	34.70	7.2	1.8	6.4	0.8	5.2	1.5	2.6
ED-18	69.30.0 N	11.15.0 W	3146	45.9	59300	32100	34.72	6.4	-0.1	5.7	0.6	4.8	0.9	2.8
ED-21	70.00.0 N	07.30.0 W	1463	14.0	28700	24600	34.89	7.0	2.2	6.1	0.8	5.2	1.9	2.1
ED-30	71.00.0 N	10.00.0 W	1097	3.4	32600	31500	34.84	5.0	1.1	3.7	-1.1	3.9	0.9	3.1
ED-37	70.33.0 N	13.15.0 W	1280	7.9	19300	17800	34.82	4.3	-0.1	2.9	-1.1	3.7	0.2	3.9
ED-38	70.30.0 N	11.15.0 W	1463	16.8	43200	35900	34.82	4.9	0.4	3.8	-1.1	4.1	0.6	3.3
ED-39	70.00.0 N	12.30.0 W	1792	35.5	68500	44200	34.78	4.9	-0.3	4.6	-1.1	3.8	0.4	3.3
ED-40	70.00.0 N	15.00.0 W	1024	11.3	22400	19900	34.70	3.8	-0.5	4.3	-1.1	3.5	0.1	3.4
ED-47	69.00.0 N	17.30.0 W	1554	17.0	41000	34000	34.20	3.2	0.0	4.8	-1.1	4.0	0.7	3.3
ED-49	69.00.0 N	14.18.0 W	1609	25.5	36700	27300	34.58	4.8	0.0	5.2	0.8	4.3	0.5	3.1
ED-51	69.00.0 N	12.30.0 W	1970	49.7	125400	63200	34.68	5.8	0.0	5.9	1.2	4.6	0.7	2.8
ED-52	68.00.0 N	12.30.0 W	1920	62.6	166100	61800	34.62	6.0	1.8	7.1	2.2	5.3	1.1	2.8
ED-53	68.00.0 N	15.00.0 W	2103	5.1	32300	30700	34.42	5.3	2.5	6.7	2.5	5.2	0.9	3.2
ED-54	68.00.0 N	17.30.0 W	1280	2.3	22300	21800	34.30	5.0	1.9	6.3	2.4	5.0	1.3	3.2
ED-55	68.00.0 N	20.00.0 W	1189	0.2	5600	5600	34.40	4.5	1.4	5.5	-0.8	4.8	1.8	2.5
ED-60	66.02.0 N	09.52.0 W	1372	7.8	36300	33500	34.65	6.9	1.7	8.7	3.1	7.0	3.0	4.8
ED-62	66.00.0 N	05.00.0 W	3292	54.4	15700	7000	34.87	8.5	3.0	9.5	3.6	8.4	4.3	6.2
ED-77	65.00.0 N	10.00.0 W	768	1.3	8800	8700	34.86	7.0	1.9	8.8	3.9	7.7	3.9	5.9
ED-87	63.00.0 N	02.30.0 W	2012	24.4	101000	76300	35.10	8.4	6.2	12.1	6.9	10.4	6.6	9.1
ED-88	63.00.0 N	05.00.0 W	2024	19.5	26100	20600	35.00	7.9	4.0	11.6	6.7	10.0	6.3	9.1
V23-58	65.46.0 N	07.07.0 W	1796	48.4	82800	42700	34.80	8.0	2.1	8.8	2.5	8.1	4.2	5.3
V23-59	68.02.0 N	00.01.0 E	3083	51.4	39700	19300	35.10	9.3	4.7	10.9	5.5	8.8	5.3	7.0
V23-74	68.11.2 N	09.36.0 W	1926	9.7	41900	37800	34.60	7.3	1.4	7.3	1.1	5.8	1.9	2.8
V23-75	64.48.0 N	01.19.0 W	2930	41.3	80900	47500	34.98	9.1	3.9	11.7	6.3	10.2	6.2	7.2
V23-76	63.39.0 N	01.22.0 E	1734	30.4	40700	28300	35.30	10.1	6.4	12.9	6.9	11.2	7.1	7.8
V27-40	63.26.9 N	06.07.8 W	1652	15.4	55000	46500	34.90	7.8	1.9	10.6	6.0	9.5	6.1	8.6
V27-46	67.35.2 N	11.31.2 W	1728	41.8	93100	54200	34.56	6.6	2.5	7.4	2.3	6.1	1.9	3.0
V27-47	68.27.7 N	13.32.5 W	1717	37.9	154600	96000	34.60	5.4	0.5	6.3	2.1	5.2	1.0	3.0
V27-53	69.32.7 N	02.49.1 W	3124	46.2	46500	25000	35.13	9.1	4.8	9.1	2.9	7.4	4.0	4.4
V27-84	68.37.7 N	01.35.7 W	3404	54.1	173200	79500	35.10	9.0	4.0	10.4	4.4	8.3	4.6	6.2
V27-93	62.56.1 N	04.16.8 E	786	24.5	15800	11900	34.00	11.7	6.0	13.6	5.6	12.1	6.7	7.3
V27-94	66.17.3 N	01.29.5 E	2781	48.7	37400	19200	35.08	10.7	6.3	12.0	6.5	10.0	6.2	8.5
V28-31	66.27.0 N	02.10.0 E	1697	32.1	34000	23100	35.10	10.8	6.8	12.1	6.4	10.2	6.4	8.6
V28-32	64.47.0 N	04.18.0 E	929	25.4	14200	10600	35.00	11.4	7.0	13.0	6.3	11.4	7.0	7.3
V28-33	62.54.0 N	00.35.0 E	1170	23.6	15700	12000	35.20	10.2	6.6	12.9	7.1	11.4	7.4	9.0
V28-35	67.07.0 N	09.34.0 W	1376	36.7	119800	75800	34.68	7.4	1.4	7.8	1.6	6.4	2.4	3.7
V28-38	69.23.0 N	04.24.0 W	3411	47.8	58800	30700	35.00	8.7	3.7	7.8	2.4	6.8	3.2	4.0
V28-39	67.53.0 N	01.56.0 W	3374	55.8	125600	55500	34.97	9.4	4.4	10.4	5.0	8.8	4.9	6.4
V28-41	67.41.0 N	00.14.0 E	3534	56.8	39600	17100	35.10	9.6	4.9	11.1	5.8	9.3	5.6	7.2
V28-42	68.05.0 N	03.51.0 E	1515	32.3	34700	23500	35.14	10.0	6.1	11.6	6.0	9.3	6.1	7.4
V28-55	65.31.0 N	00.12.0 E	2886	47.2	89200	47100	35.02	10.3	4.4	11.9	6.6	10.3	6.2	7.6
V28-56	68.02.0 N	06.07.0 W	2941	52.2	31800	15200	34.90	8.2	3.2	8.4	2.2	6.7	2.8	4.2
V28-59	64.52.0 N	07.52.0 W	2622	38.4	92700	57100	34.78	6.9	1.8	8.9	3.4	8.7	5.1	6.1
V28-60	64.05.0 N	04.02.0 W	3244	47.7	102100	53400	34.86	8.1	2.4	10.9	4.4	9.4	5.6	8.1
V28-60A	64.25.0 N	04.02.0 W	3231	51.0	113900	55800	34.85	8.1	2.2	10.4	4.1	9.4	5.6	7.8
V29-209	65.36.0 N	06.29.0 W	2698	50.8	47800	23500	34.78	8.0	2.2	9.0	2.9	8.3	4.4	5.6
V29-210	66.44.0 N	06.44.0 W	2460	55.9	42900	18900	34.80	8.1	2.3	8.8	2.4	7.8	3.8	4.8



Table 2 (continued)

Station	Latitude	Longitude	Depth (m)	CaCO <sub>3</sub> (%)	Rads/gr CaCO <sub>3</sub> free	Rads/gr Die	Sal Die	ST Die	WT Die	ST Kel	WT Kel	ST Lev	WT Lev	ST ICE
V30-132	65.04.0 N	07.08.0 W	2028	51.5	65700	31900	34.76	7.2	1.8	9.1	3.0	8.1	4.2	6.0
V30-133	65.08.0 N	05.18.0 W	3843	37.8	47900	29900	34.80	8.0	1.9	9.6	3.5	8.6	4.7	6.5
V30-135	70.18.0 N	09.33.0 W	1308	18.9	48200	39100	34.84	6.2	1.8	5.1	-0.8	4.6	1.2	2.6
V30-167	67.00.0 N	05.51.0 E	1348	23.5	23200	17700	35.03	10.6	6.9	12.3	6.2	10.2	6.8	7.8
V30-169	67.30.0 N	05.51.0 E	1439	24.9	20000	15100	35.00	10.4	6.6	12.1	6.3	10.2	6.8	7.7
V30-170	67.16.0 N	07.01.0 E	1363	26.6	18500	13600	34.90	10.0	6.9	12.3	6.0	10.3	7.0	7.6
V30-175	67.51.0 N	05.46.0 E	1383	36.7	42700	27100	35.05	10.3	6.5	11.9	6.1	10.2	6.8	7.5
HM31-35	64.32.0 N	01.14.0 E	2750	43.7	71500	40300	35.12	10.4	6.0	12.6	7.1	10.2	6.2	7.4
HM31-37	63.46.7 N	0.00.0 E	2285	21.7	13200	10300	35.10	9.6	5.5	12.4	7.3	11.0	7.0	7.7
V29-211	67.47.0 N	06.40.0 W	2553	55.9	38100	16800	34.85	8.0	3.0	8.6	2.0	7.3	3.2	4.0
V29-219	68.23.0 N	05.27.0 W	3384	55.4	98700	44000	35.00	8.5	3.4	8.3	2.5	7.0	3.2	4.3
V29-220	65.10.0 N	00.04.0 W	2873	33.1	52900	35400	35.03	10.2	4.3	11.8	6.6	10.0	6.0	7.2
V30-130	67.30.0 N	15.04.0 W	858	1.1	10000	9800	34.40	6.1	3.6	7.3	3.2	6.2	1.4	3.4
V30-131	66.51.0 N	09.02.0 W	1595	47.2	72700	38500	34.70	7.5	1.6	8.3	1.6	7.0	3.0	4.0

Number of radiolarians per gram CaCO<sub>3</sub> free sediment and number of radiolarians per gram bulk sediment have been rounded to the nearest hundred.

and northern (173 000 skeletons/g at station V27-84) parts of the Norwegian Basin. The number of radiolarian skeletons per gram carbonate-free sediment is lower in the hemipelagic sediments on the upper part of the continental slope, close to the continents (shallower than ca. 1000 m).

The 11 species most commonly encountered in the surface sediments of the GIN Seas were:

(1) Spumellarida: *Actinomma boreale*\*, *A. leptoderma*\*, *Larcospira minor*, and *Phortidium clevei*.

(2) Nassellarida: *Amphimelissa setosa*\*, *Arto botrys boreale*\*, *Lithomelissa setosa*\*, *Lithocampe platycephala*\*, *Pseudodictyophimus gracilipes*\*, *Cycladophora davisiana* and *Lithomitra lineata*.

Distribution maps are given for the most common of these species, marked with an asterisk.

The distribution of all 11 most common species are discussed below, including comparison of distribution data from other authors:

*Amphimelissa setosa* (Fig. 5) is, according to Bjørklund and Swanberg (1987), present in two morphological varieties in the study area, a “reticulate neritic” (12% and 33% of the *A. setosa* population in the plankton and surface sediments on the Iceland Plateau respectively) and a “smooth oceanic” form. Both forms were encountered during the present study. The smooth oceanic form is known for its cold water affinity, with the reticulate form becoming dominant over the smooth form going eastward

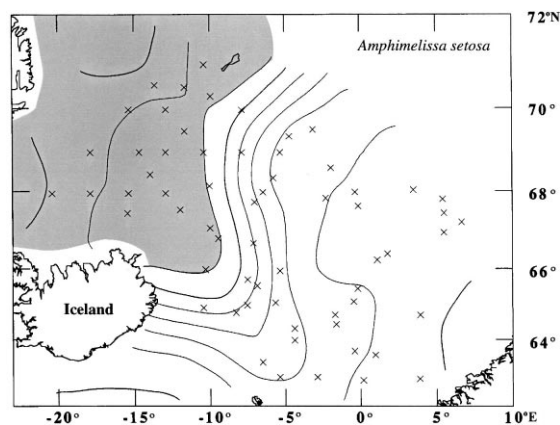


Fig. 5. Distribution map for the relative percentages of *Amphimelissa setosa*. This species has a scaled varimax factor score of 5.269 in Factor 1. Areas where the relative percentages of *Amphimelissa setosa* are higher than 60% are shaded. Increment between isolines = 10; heavy line increment = 50.

towards the western coast of Norway and into the fjords. However, the total number of *A. setosa* (regardless of the form) in the sediments decreases from west to east. This is supported by its distribution in the western part of the GIN Seas, being dominant (up to 76%) at the Iceland Plateau and common (>20%) just north of the Iceland–Faeroe Ridge, Fig. 5. This closely parallels with the extent of water masses having a surface temperature colder than 10°C during the summer (Fig. 2b).

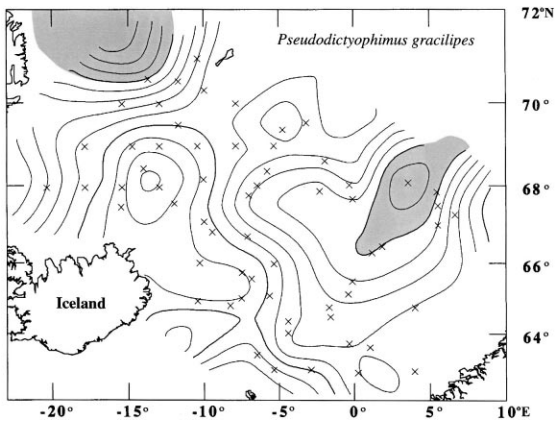


Fig. 6. Distribution map for the relative percentages of *Pseudodictyophimus gracilipes*. This species has a scaled varimax factor score of 3.247 in Factor 2. Areas where the relative percentages of *Pseudodictyophimus gracilipes* are higher than 15% are shaded. Increment between isolines = 1; heavy line increment = 5.

*Pseudodictyophimus gracilipes* (Fig. 6) had its main distribution in the eastern GIN Seas, largely reflecting the presence of Atlantic water and the mixing area of warm and cold water southeast of Jan Mayen, with a maximum of 21% at the junction of the Lofoten and Norwegian Basins. It also occurred in the proximity of the ice edge offshore of Greenland, Fig. 6, in agreement with the observations of Swanberg and Eide (1992), who found this species at all of their stations.

*Lithomelissa setosa* (Fig. 7) had warm water affinity and is the most common species in the eastern part of the Norwegian Sea (16%), especially common in the Atlantic domain and in the central gyre of warm and cold water mixing, traced by the 5% isoline in Fig. 7. In the Iceland Sea *L. setosa* is only found as trace abundances, <1%.

*Actinomma boreale* and *A. leptoderma* (Fig. 8a–c) are usually reported as a group (e.g. Samtleben et al., 1995), due to difficulty in identification, particularly of juvenile stages. In Fig. 8a the abundance of the *Actinomma* sp. group is plotted, showing high percentages to the east of a line drawn from Jan Mayen to the Faeroe Islands, as shown by the 9–10% isoline. However, the area located between the summer and winter positions of the sea ice-edge, also showed a slight increase in the relative abundance of the *Actinomma* sp. group. By applying the species con-

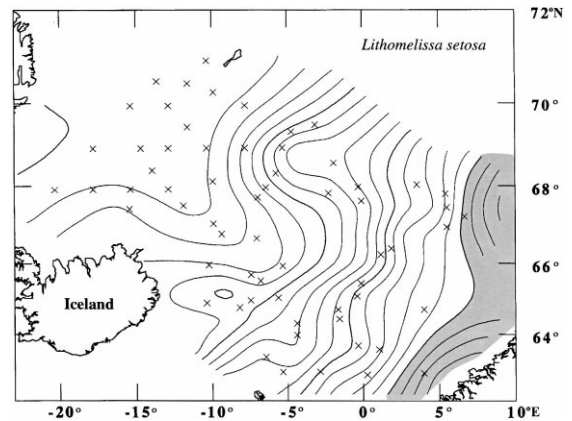


Fig. 7. Distribution map for the relative percentages of *Lithomelissa setosa*. This species has a scaled varimax factor score of 2.731 in Factor 2 and -2.176 in Factor 3. Areas where the relative percentages of *Lithomelissa setosa* are higher than 15% are shaded. Increment between isolines = 1; heavy line increment = 5.

cepts of Cortese and Bjørklund (1998) we were able to recognize two species.

The *Actinomma boreale* distribution (Fig. 8b) was limited to the eastern part of the GIN Seas. It was particularly abundant, >7%, in the area east of 0° longitude, with a branch extending westward at 68°N latitude.

*A. leptoderma* was most abundant between 0 and 10°W, Fig. 8c, with two distinct distribution maxima, one in the northern and one in the central part of the Norwegian Basin. These two maxima were intersected by the Arctic Front, the northern being to the west of the front, whilst the southern was on the eastern side. In addition, the relative abundances of *A. leptoderma* increased towards the ice-edge off Greenland, Fig. 8c. This observation is also in accordance with those of Swanberg and Eide (1992), who found *A. leptoderma* to be one of the dominant species of living plankton in that area.

In their studies of the polycystine radiolarian distributions in the western Iceland and southern Greenland Seas, Molina-Cruz and Bernal-Ramirez (1996) could not identify any clear pattern in the distributions of *A. boreale* and *A. leptoderma*. However, they reported these species at their highest abundances where Arctic Surface Water was present. The percentage abundance values of these species are approximately the same as those in our estimates.

*Lithocampe platycephala* (Fig. 9) was present at all stations. Its 8% isoline corresponded well with the deepest part of the Norwegian Basin. We associated this distribution with the area east of the gyre where the cold East Iceland Current and the warm

Norwegian Current mix. *L. platycephala* was also present in high percentages in the ice edge area between Greenland and Jan Mayen, in close agreement with Molina-Cruz and Bernal-Ramirez (1996). However, the latter authors encountered *L. platycephala* in abundances from 11.3 to 18.7% of the fauna, values twice as high as those we found.

*Artobotrys boreale* (Fig. 10) distribution was centered in the eastern part of the GIN Seas, with particularly high percentages (up to 11%) in the northern Norwegian Basin, but also in the central Norwegian Basin, with maximum occurrences in the GIN Seas to the east of the mixing zone of warm and cold water. Its geographical distribution suggests that it is confined to high northern latitudes, both in the Pacific and Atlantic Oceans (Kruglikova, 1977), and as such it is interpreted as a cold water species.

High abundances of *Phorticium clevei* were found in the area east of the Arctic Front, under the influence of Atlantic water. The highest percentage (10%) was found in the northwestern Norwegian Basin. This species had low occurrences in the Iceland Sea, <1%, in very good agreement with the results of Molina-Cruz and Bernal-Ramirez (1996).

*Larcospira minor* percentages showed a distinct gradient of abundance increasing from the west to the east. This gradient steepened and reached particularly high values (8–10%) on the Vøring Plateau in the easternmost portion of the study area.

*Lithomitra lineata* had the same distribution pattern as *Artobotrys boreale*, with maxima (7%) both

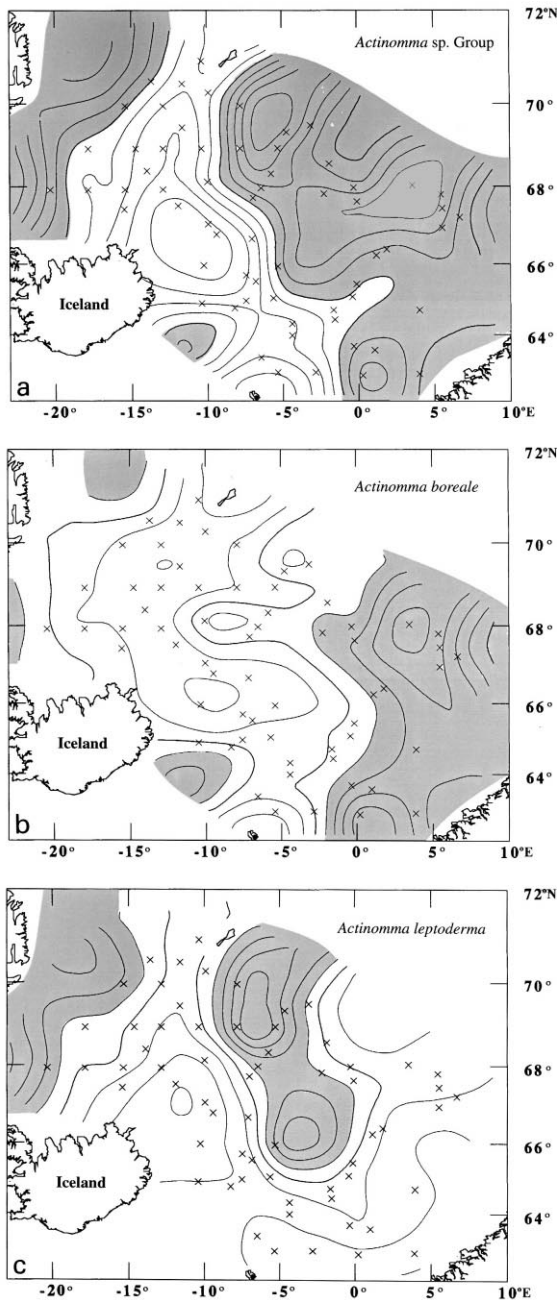


Fig. 8. (a) Distribution map for the relative percentages of *Actinomma* 'group' (*A. boreale* and *A. leptoderma*). Areas where the relative percentages of *Actinomma* 'group' are higher than 10% are shaded. Increment between isolines = 1; heavy line increment = 5. (b) Distribution map for the relative percentages of *Actinomma boreale*. This species has a scaled varimax factor score of 1.851 in Factor 2 and -1.193 in Factor 3. Areas where the relative percentages of *Actinomma boreale* are higher than 6% are shaded. Increment between isolines = 1; heavy line increment = 5. (c) Distribution map for the relative percentages of *Actinomma leptoderma*. This species has a scaled varimax factor score of 1.994 in Factor 3. Areas where the relative percentages of *Actinomma leptoderma* are higher than 6% are shaded. Increment between isolines = 1; heavy line increment = 5.

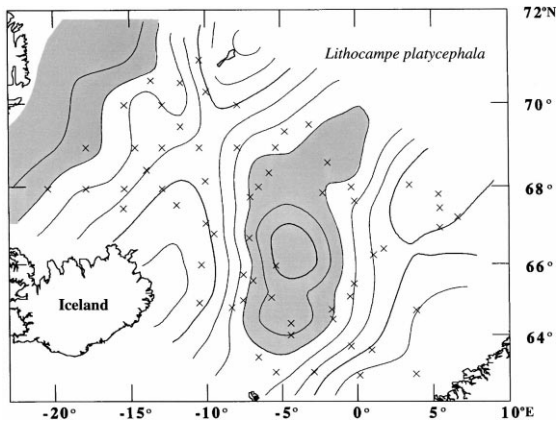


Fig. 9. Distribution map for the relative percentages of *Lithocampe platycephala*. This species has a scaled varimax factor score of 1.133 in Factor 2 and 3.215 in Factor 3. Areas where the relative percentages of *Lithocampe platycephala* are higher than 8% are shaded. Increment between isolines = 1; heavy line increment = 5.

in the northern and in the central Norwegian Basin. According to Boltovskoy (pers. comm. 1997), a closely related species (*L. arachnea*) dominates southern polar waters and their associated sedimentary assemblages. This implies high standing stocks of living populations, most probably associated with levels of maximum radiolarian abundance (Boltovskoy, pers. comm. 1997). In the Labrador Sea ODP Site 646, *L. lineata* has peak occurrences in the

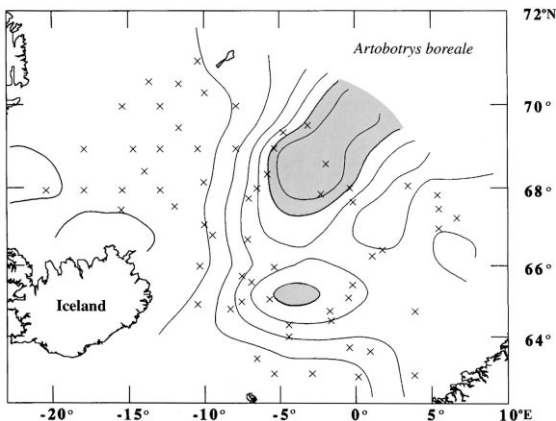


Fig. 10. Distribution map for the relative percentages of *Artobotrys boreale*. This species has a scaled varimax factor score of 1.504 in Factor 3. Areas where the relative percentages of *Artobotrys boreale* are higher than 5% are shaded. Increment between isolines = 1; heavy line increment = 5.

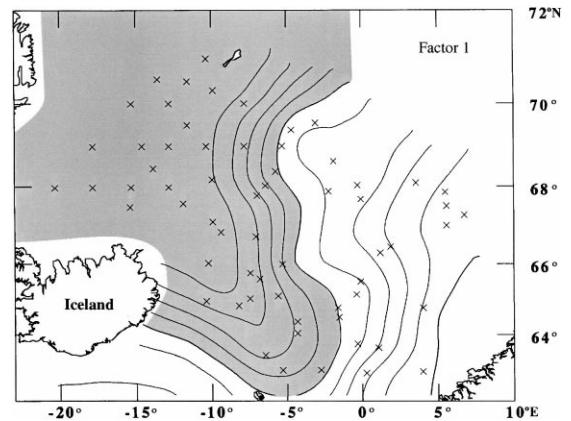


Fig. 11. Geographical distribution of factor components for Factor 1. The most important species for this factor is *Amphimelissa setosa*, with a scaled varimax factor score of 5.269. Areas where factor components for Factor 1 are higher than 0.500 are shaded. Increment between isolines = 0.100; heavy line increment = 0.500.

Plio-Pleistocene sediments (Bjørklund, unpublished data), indicating the potential use of this species in palaeoecological interpretations. In the Norwegian Basin *L. lineata* is most abundant in the mixing zone of warm and cold water.

*Cycladophora davisiana* occupied the central part of the Norwegian Basin with percentages higher than

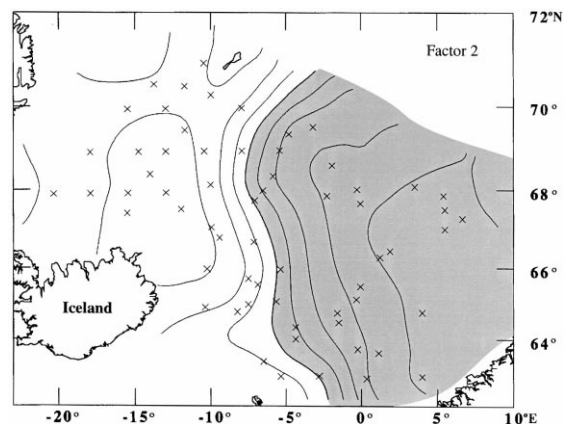


Fig. 12. Geographical distribution of factor components for Factor 2. The most important species for this factor are *Pseudodictyophimus gracilipes* (3.247), *Lithomelissa setosa* (2.731) and *Actinomma boreale* (1.851), scaled varimax factor score in brackets. Areas where factor components for Factor 2 are higher than 0.500 are shaded. Increment between isolines = 0.100; heavy line increment = 0.500.

Table 3  
Varimax factor components matrix (station vs. factors)

Stations	Comm.	Factor 1	Factor 2	Factor 3
ED-14	0.882	0.313	0.801	0.378
ED-15	0.878	0.690	0.527	0.352
ED-17	0.998	0.985	0.157	0.056
ED-18	0.999	0.985	0.153	0.067
ED-21	0.979	0.954	0.238	0.114
ED-30	0.996	0.987	0.143	0.036
ED-37	0.975	0.924	0.332	0.106
ED-38	0.992	0.955	0.251	0.133
ED-39	0.996	0.983	0.165	0.058
ED-40	0.991	0.968	0.210	0.098
ED-47	0.997	0.974	0.193	0.103
ED-49	0.996	0.975	0.186	0.102
ED-51	0.998	0.991	0.117	0.049
ED-52	0.999	0.991	0.112	0.062
ED-53	0.997	0.974	0.203	0.080
ED-54	0.999	0.980	0.186	0.063
ED-55	0.981	0.933	0.306	0.128
ED-60	0.996	0.981	0.178	0.027
ED-62	0.910	0.293	0.643	0.641
ED-77	0.991	0.974	0.204	-0.028
ED-87	0.966	0.912	0.363	-0.036
ED-88	0.989	0.945	0.297	0.088
V23-58	0.995	0.980	0.176	0.062
V23-59	0.935	0.501	0.760	0.326
V23-74	0.987	0.974	0.195	0.011
V23-75	0.920	0.552	0.728	0.294
V23-76	0.942	0.260	0.931	0.083
V27-40	0.962	0.913	0.357	0.018
V27-46	0.998	0.992	0.116	0.021
V27-47	0.991	0.991	0.073	0.054
V27-53	0.946	0.327	0.849	0.345
V27-84	0.940	0.418	0.814	0.319
V27-93	0.876	-0.002	0.914	-0.203
V27-94	0.931	0.287	0.912	0.131
V28-31	0.961	0.143	0.966	-0.093
V28-32	0.923	-0.002	0.952	-0.133
V28-33	0.927	0.057	0.947	-0.167
V28-35	0.998	0.990	0.133	0.018
V28-38	0.922	0.237	0.900	0.234
V28-39	0.910	0.342	0.852	0.257
V28-41	0.935	0.329	0.888	0.197
V28-42	0.926	0.084	0.952	-0.116
V28-55	0.966	0.557	0.806	0.081
V28-56	0.953	0.508	0.765	0.332
V28-59	0.984	0.901	0.403	0.099
V28-60	0.975	0.702	0.661	0.188
V28-60A	0.955	0.743	0.579	0.261
V29-209	0.919	0.783	0.449	0.322
V29-210	0.986	0.885	0.395	0.218
V29-211	0.975	0.814	0.509	0.230
V29-219	0.957	0.378	0.859	0.276
V29-220	0.933	0.507	0.818	0.079
V30-130	0.998	0.984	0.169	0.026

Table 3 (continued)

Stations	Comm.	Factor 1	Factor 2	Factor 3
V30-131	0.998	0.990	0.133	0.016
V30-132	0.987	0.957	0.256	0.081
V30-133	0.962	0.763	0.576	0.221
V30-135	0.997	0.984	0.164	0.025
V30-167	0.978	0.052	0.987	-0.042
V30-169	0.932	0.057	0.958	-0.108
V30-170	0.828	0.033	0.908	-0.048
V30-175	0.973	0.041	0.965	0.065
HM31-35	0.947	0.328	0.908	0.122
HM31-37	0.937	0.702	0.662	0.075
Variance		56.08	36.60	3.39
Cum. variance		56.08	92.69	96.07

3%, and maximum values of ca. 6% in the central part of the basin. Petrushevskaya (1967), Morley and Hays (1979), and Bjørklund and Ciesielski (1994) demonstrated this species to be a deep and cold water indicator. The stratigraphical distribution of *C. davisiana* displays a significant peak occurrence in the North Atlantic (Morley, 1983). This peak has been correlated to the last glacial maximum, therefore making this species a high resolution biostratigraphical tool at both high northern and southern latitudes.

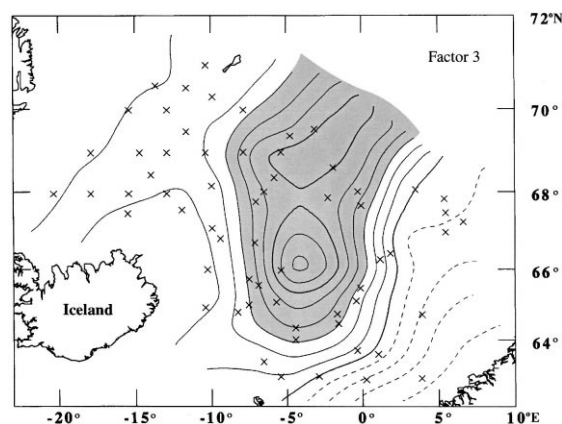


Fig. 13. Geographical distribution of factor components for Factor 3. The most important species for this factor are *Lithocampe platycephala* (3.215), *Lithomelissa setosa* (-2.176) *Actinomma leptoderma* (1.994) and *Artobotrys boreale* (1.504), scaled varimax factor score in brackets. Areas where factor components for Factor 3 are higher than 0.150 are shaded. Increment between isolines = 0.050; heavy line increment = 0.300.

Table 4  
Scaled varimax factor scores matrix (species vs. factor scores)

Species	Factor 1	Factor 2	Factor 3
<i>Actinomma boreale</i>	0.017	<b>1.851</b>	<b>-1.193</b>
<i>Actinomma leptoderma</i>	-0.011	0.924	<b>1.994</b>
<i>Amphimelissa setosa</i>	<b>5.269</b>	0.112	-0.066
<i>Artobotrys boreale</i>	-0.205	0.868	<b>1.504</b>
<i>Artostrobos annulatus</i>	0.009	0.060	0.277
<i>Artostrobos joergenseni</i>	0.058	0.348	0.152
<i>Corocalyptra craspedota</i>	-0.060	0.346	-0.270
<i>Cycladophora davisiana</i>	-0.023	0.558	<b>1.202</b>
<i>Euphysetta nathorstii</i>	0.031	0.107	0.203
<i>Hexacantium pachydermum</i>	-0.010	0.123	-0.261
<i>Larcospira</i> sp. 1	-0.059	0.459	-0.448
<i>Larcospira minor</i>	-0.131	0.885	-0.410
<i>Lipmanella xipheporum</i>	-0.022	0.105	-0.007
<i>Lirella melo</i>	0.045	0.087	0.215
<i>Lithelius spiralis</i>	-0.015	0.123	-0.159
<i>Lithocampe platycephala</i>	0.123	<b>1.133</b>	<b>3.215</b>
<i>Lithomelissa hystrix</i>	-0.038	0.337	-0.416
<i>Lithomelissa setosa</i>	-0.229	<b>2.731</b>	<b>-2.176</b>
<i>Lithomitra lineata</i>	-0.058	0.249	<b>1.084</b>
<i>Peridium longispinum</i>	0.009	0.035	-0.036
<i>Phorticium clevei</i>	-0.235	<b>1.101</b>	<b>1.140</b>
<i>Plectacantha oikiskos</i>	0.002	0.125	0.140
<i>Pseudodictyophimus gracilipes</i>	0.166	<b>3.247</b>	-0.015
<i>Rhizoplegma boreale</i>	-0.057	0.240	0.266
<i>Spongotrochus glacialis</i>	-0.053	0.421	-0.257
<i>Streblacanta</i> sp. 1	-0.029	0.222	-0.196
<i>Stylodictya validispina</i>	-0.031	0.318	-0.395
<i>Tholospyris gephristes</i>	0.014	0.515	0.313

Absolute values of factor scores higher than one are indicated in bold typeface.

#### 4.2. Factor analysis of radiolarian associations

The dataset (Appendix B), species counts in stations, was used to group the species into various associations by applying the CABFAC factor analysis technique.

The resulting varimax factor components (Table 3) are plotted by stations in a set of maps (Figs. 11–13) to represent visually the factors extracted.

We have interpreted Factor 1 (Fig. 11) as a cold (Polar and Arctic) water factor, because high (>0.90) factor loadings are found on the Iceland Plateau, and the 0.50–0.60 isolines roughly trace the position of the Arctic Front and the intrusion of the cold East Iceland Current towards the southern sector of the Norwegian Basin. *Amphimelissa setosa* dominated

this factor with a varimax factor score of 5.269, Table 4.

Factor 2 (Fig. 12) has been interpreted as a warm (Atlantic) water factor, with particularly high (>0.80) factor loadings on the Vøring Plateau. The warm Norwegian Current sends off a gyre to the northwest, which reaches just to the southeast of Jan Mayen. This gyre is visible in the lobate shape of the isolines of the factor loadings of Factor 2 (Fig. 12).

Species with a high varimax factor 2 score included *Pseudodictyophimus gracilipes* (3.247), *Lithomelissa setosa* (2.731) and *Actinomma boreale* (1.851), Table 4.

Factor 3 (Fig. 13) was best described as a central Norwegian Basin factor as factor loadings higher than 0.20 reproduced well the shape of this basin, including the protrusion of the Vøring Plateau from the east to the west. We associate this pattern with the gyre where the cold East Greenland Current and the warm Norwegian Current mix. High absolute values of varimax scores were obtained for *Lithocampe platycephala* (3.251), *Lithomelissa setosa* (-2.176), *Actinomma leptoderma* (1.994) and *Artobotrys boreale* (1.504), Table 4.

## 5. Discussion

### 5.1. Correlation of factor analysis with environmental parameters

Marine micropalaeontological investigations that have attempted to use proxies to extrapolate to ecological information about past environments have generally correlated microfossil distributions with modern sea-surface temperature (or occasionally salinity) and related this downcore to palaeotemperatures. Often this has been because the palaeoecological investigations have been interested primarily in temperature as an indication of general palaeoenvironmental conditions, but it is probably often the case that temperature and salinity are the parameters that are easiest to obtain over a wide range of space and time. Temperature is certainly important to living organisms, and controls their distribution in a very broad sense (they tend to be related to water masses), but one must keep in mind that species, not assemblages, respond to their environment, and that most species of plants and animals have a gaussian response to temperature (see

lengthy discussion of multivariate analysis in Gauch, 1982, and references therein) and most other environmental variables. Factor analysis elaborates the correlation between the species distributions and the parameters in question. The assumptions of factor analysis depend on a linear response by species to the variables being investigated (Gauch, 1982). This means that factor analysis will work quite well as a linear estimate of regions of a gaussian curve over short gradients. End members (extreme differences related to water masses) certainly appear strongly, but are probably much less sensitive in extracting reliable equations. Factor analysis should be less useful in areas where there are long gradients in the parameter in question. The traditions in paleoecology and ecology are totally different in this area: few modern multivariate ecological investigations use factor analysis.

The distributions of plants and animals are influenced by a number of other environmental parameters, which should serve to blur the temperature signal. In particular, animals and plants are all dependent on nutrition, either from sunlight and nutrients in the case of autotrophs or from other organisms in the case of heterotrophs. This means that the general ecological conditions of the surrounding marine community probably has more effect on species distributions than does temperature. Temperature should be considered as a necessary but not sufficient parameter for most organisms' survival. Changes in temperature regimes can exclude species, or permit them to invade new areas if all other conditions permit. That many species distributions correlate well with temperature is probably more an indication of the fact that water masses, and all of the more provincial biologic factors controlling taxa, correlate well with temperature, than that temperature has some direct tight mechanistic control on species distribution. Hence uncritical extrapolation of present day temperature correlations into the geological past is perilous.

When analyzing the faunal assemblages in an area, it is of interest to seek correlation with oceanographic parameters such as temperature, salinity, phosphate, nitrate, nitrite, silica, chlorophyll, phaeopigment. We tested the relationship between the different factor scores and various oceanographic datasets.

Sea surface temperature data sets are essentially of two kinds: those collected almost simultaneously, synoptical data (Dietrich, 1969), and those that have

been collected over many years and during different seasons (USNHO, 1958; USNOO, 1967; Kellogg, 1975; Levitus, 1982; ICES, 1996).

Dietrich (1969) gives a more accurate picture of the position of both water masses and fronts in the GIN Seas. Levitus (1982), and also the other non-synoptic data sets, instead show a simple west-east temperature gradient with parallel isotherms, and do not reflect major oceanographic features such as the East Iceland Current and the westward branch of the Norwegian Current.

This is also in accordance with the conclusion by Sarnthein and Altenbach (1995): "The Levitus SST data that form the calibration base of both the SIM-MAX and CABFAC transfer techniques for deducing paleotemperatures contain a further, widely unrecognized problem in the Nordic Seas. These SST values average the measured data over large regions and many decades, thus they would suppress the actual oceanographic frontal systems and are much too high in the close vicinity of sea-ice margins in the Greenland Sea (2.5–4.0°C) compared with synoptic (real) SST distribution patterns (0–2°C). If these Levitus SST data are used as boundary conditions of three-dimensional circulation models, they even suppress major features such as the East Greenland Current (Seidov et al., submitted). To overcome this problem, Seidov et al. (submitted) have adjusted the Levitus average values off Greenland to the genuine synoptic SST data of Dietrich (1969)".

But sediment top distributions of radiocesium are not synoptical. They are time averaged. Hence, a priori we might expect the non-synoptic datasets to give better correlation if temperature actually controlled distribution. Better correlation with Dietrich dataset thus may support the hypothesis that temperature per se is not the real control, but simply an indicator of oceanographic conditions.

The discussion above made us prefer, for correlation purposes, the synoptical Dietrich (1969) data set rather than any other more recent non-synoptical temperature data set (as Kellogg, 1975; Levitus, 1982; ICES, 1996).

The correlation coefficients between Factors 1 to 3 and the four datasets of sea surface temperature were calculated and are shown in Fig. 14. The synoptical data from Dietrich show a very good correlation ( $R^2 = 0.835$ ) to our Factor 1, as well as to Factor 2

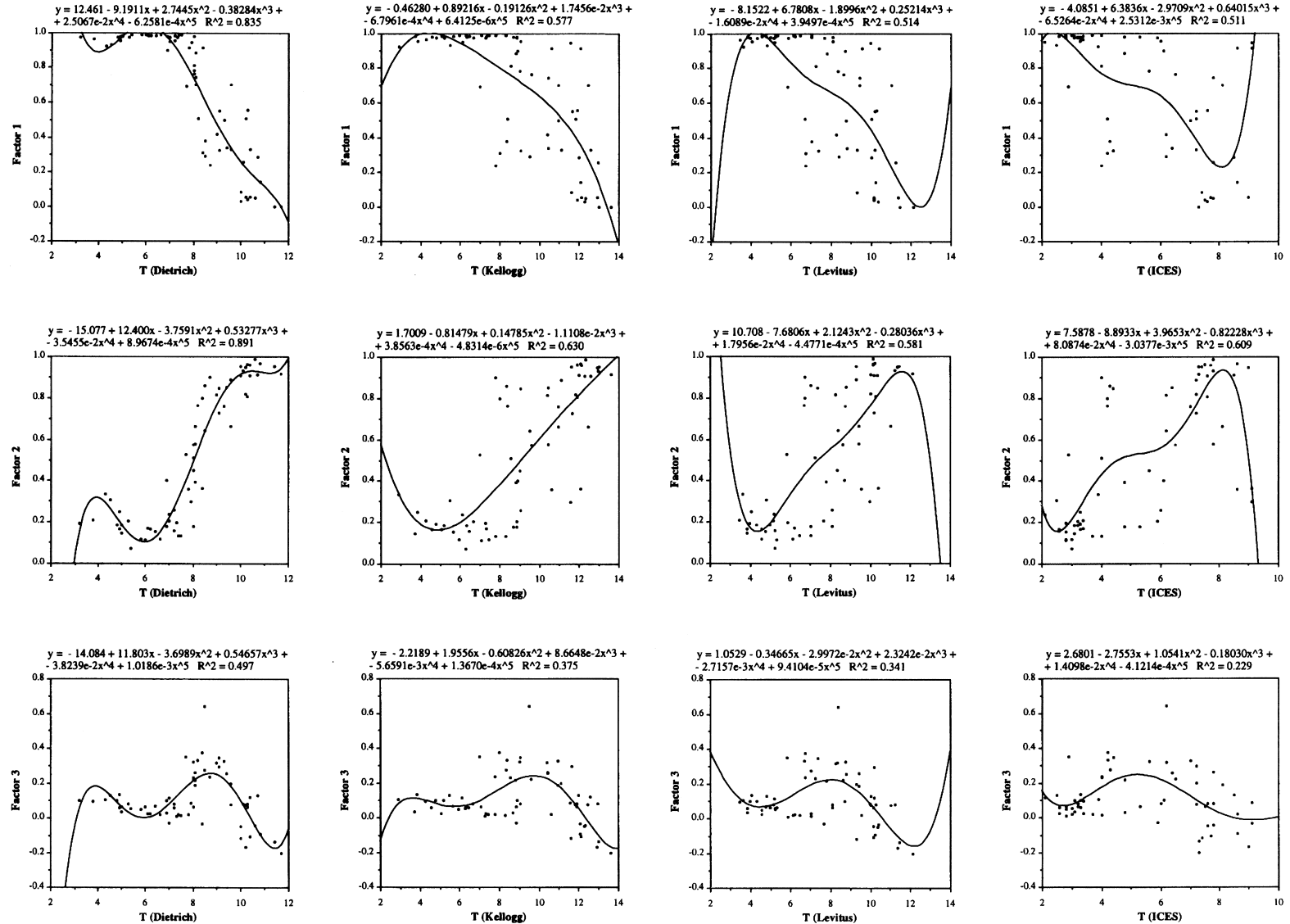


Fig. 14. Correlation between the factor component values for the first three factors recognized in this study and the corresponding summer sea surface water temperature values as available from four different datasets (Dietrich, 1969; Kellogg, 1975; Levitus, 1982; ICES, 1996). Fifth degree polynomial interpolation has been used.



( $R^2 = 0.891$ ), which is apparent from the plots in Fig. 14, while Factor 3 ( $R^2 = 0.497$ ) shows a worse correlation to temperature, however still significant at the 5% confidence level. The other data sets do show the same trend, with Factor 1 and 2 probably related to temperature, or to unknown parameters related to temperature, while Factor 3 is more loosely correlated to temperature.

Table 5

Correlation coefficients between Factors 1 to 3 and temperature, salinity, phosphate, silicate and nitrate from 0, 20, 50, 100 and 200 m depths

Depth (m)	Factor 1	Factor 2	Factor 3	Stations
<i>Temperature</i>				
0	0.511	0.609	0.229	385
20	0.528	0.631	0.334	335
50	0.575	0.702	0.505	340
100	0.614	0.729	0.572	323
200	0.646	0.706	0.583	263
<i>Salinity</i>				
0	0.337	0.530	0.085	368
20	0.402	0.587	0.081	335
50	0.723	0.905	0.163	340
100	0.601	0.782	0.248	323
200	0.595	0.661	0.316	263
<i>Phosphate</i>				
0	0.478	0.617	0.092	355
20	0.428	0.558	0.096	332
50	0.432	0.618	0.188	317
100	0.389	0.552	0.152	302
200	0.149	0.212	0.073	260
<i>Silica</i>				
0	0.391	0.523	0.312	398
20	0.254	0.360	0.281	307
50	0.265	0.402	0.108	295
100	0.137	0.241	0.028	277
200	0.304	0.221	0.044	208
<i>Nitrate</i>				
0	0.281	0.387	0.167	198
20	0.379	0.397	0.212	241
50	0.199	0.200	0.191	232
100	0.056	0.051	0.152	215
200	0.128	0.165	0.058	157

Oceanographic data from ICES (1996). The right column gives the number of stations that has been used to produce a map of the distribution of each parameter at the different depths. These maps were used to extrapolate the values of the different parameters corresponding to the geographical position of our 63 stations.

We also calculated the correlation coefficients for the three factors against the temperature reported in the ICES database for depths of 0, 20, 50, 100, and 200 m (Table 5). All the correlations between our factors and ICES temperatures were significant at the 5% confidence level, and there was a trend of improving correlation coefficients with depth, with the best fit at 200 m for Factors 1 and 3 and at 100 m for Factor 2, an increase of ca. 0.35 in the correlation coefficient for Factor 3.

Petrushevskaya (1971) reported that the bulk of living radiolarians in the open Pacific Ocean was found between 100 and 200 m. Swanberg and Bjørklund (1986) also documented that radiolarians in west Norwegian fjords had peak occurrences at subsurface depths, and finally Swanberg and Eide (1992) reported that radiolarians from the east Greenland Sea had their highest concentrations below 25 m. We therefore concluded that if there were a correlation between the radiolarian assemblages and temperature, we had to test this relationship with temperature at the depth where radiolarians are most likely to live. The fact that salinity and temperature correlation coefficients increase with depth indirectly confirms that the optimal living depth for radiolarians is not at the surface, but deeper.

We then correlated the Dietrich (1969) temperature data from 0, 50, 100, and 200 m for both winter and summer (Table 6) with our Factors 1–3. These observations are in accordance to the find-

Table 6

Correlation coefficients between Factors 1 to 3 and winter and summer temperatures at 0, 50, 100 and 200 m depths

Depth (m)	Factor 1	Factor 2	Factor 3
<i>Winter</i>			
0	0.771	0.762	0.460
50	0.827	0.865	0.603
100	0.856	0.875	0.590
200	0.811	0.818	0.527
<i>Summer</i>			
0	0.835	0.891	0.497
50	0.642	0.702	0.398
100	0.673	0.754	0.563
200	0.758	0.777	0.517

Data from Dietrich (1969).

ing of mesoscale eddies along the southern portion of the Arctic Front (Niiler et al., 1992). These eddies are short ranging in time, have a very local distribution and only limited to the upper 50 m, making the deeper parts of the water column and the position of the Arctic Front more stable. This could therefore explain the increasingly better correlation of temperature and radiolarian associations with depth.

A trend of better correlation was evident for winter temperatures and Factors 1 and 2 with increasing depth, being optimal at 100 m. For the summer, however, the best fit was found for the surface values. For Factor 3 there was a looser correlation to temperature, but the results show that at 50 and 100 m, in winter and in summer respectively, the correlation coefficient for Factor 3 reaches its highest value.

The ICES (1996) data also provided information on temperature, salinity, silicate, phosphate, and nitrate from hundreds of stations in the GIN Seas.

In our analysis of the data the correlation coefficients ( $r^2$ ) between factor scores and salinity, silicate, phosphate, and nitrate are significant at the 5% confidence level (for  $n = 62$  then  $r = 0.25$  or higher, i.e.  $r^2 = 0.06$  or higher, is significant at the 5% confidence level) at any depth. The only exceptions (Table 5) were Factor 3 vs. silicate at 200 m depth, Factor 1 and Factor 2 vs. nitrate at 100 m depth, and Factor 3 vs. nitrate at 200 m depth. For nitrite, pH, and ammonium data were not available from a large enough number of stations to correlate these parameters to our factor scores.

The correlation between radiolarian associations (factors) and nutrient content (dissolved phosphate, silicate and nitrate of seawater) decreases with depth. This can be interpreted as caused by the fact that radiolarians are mainly feeding on primary producers, therefore there is an indirect correlation with nutrients (Table 5).

In neritic waters on the west coast of Norway, Bjørklund (1973) reported a mid-summer radiolarian abundance peak, following the spring phytoplankton bloom and copepod abundance peak. This is also in agreement with the general biological assumption that individuals reproduce when food is available. In the Greenland Sea, Swanberg and Eide (1992) concluded that nassellarians mostly fed on nanoflagellates and small ciliates. They also reported that the

upper 25 m were not sampled due to clogging of the net by phytoplankton and that the highest concentrations were found below this zone of phytoplankton production, with densities between 4.58 and 69.92 radiolarians/ $m^3$  (stations PS 83 and EN 6, respectively), a rather low number when compared to the neritic value of 2000 radiolarians/ $m^3$ , reported by Swanberg and Bjørklund (1986).

We do not have any radiolarian plankton abundance data for the winter in the GIN Seas. However it is likely that they would be lower, as both Bjørklund (1973) and Swanberg and Bjørklund (1986) demonstrated low radiolarian abundances in the neritic waters of western Norway during winter. In the Subarctic Pacific the radiolarian flux displays peak values from April to September 1983 and from April to August 1984, while low flux values are found in the winter (Takahashi, 1987).

Factors 1 and 2 probably correlated better with summer than with winter surface temperature, Table 6, because the reproduction of polycystine radiolarians occurs in the summer, which is also the season for phytoplankton production, one of the assumed food sources for polycystine radiolarians. The bulk of the skeletons would therefore be produced in the water column and transported to the surface sediments during this season.

Very high correlation values between temperature and factor scores are found for the winter temperature dataset at 50, 100 and 200 m depths, Table 6. Our working hypothesis for this good correlation is that it is in the winter that the cold water lobe southeast of Iceland is more evident. In this season the East Iceland Current, carrying ASW, reaches its easternmost position. Since the radiolarian assemblage of this watermass is dominated by *Amphimelissa setosa* and since this species is one of the most common in the study area, this eastward migration of the Arctic Front allows it to settle down in the bottom sediments in areas where this species is most probably not present in the plankton in summer.

## 5.2. Factor analysis, abundance and association patterns

There appear to be three areas high in radiolarian abundance in the GIN Seas (Fig. 4). (1) The southernmost of the three areas of high radiolarian



Table 7  
Chlorophyll *a* measurements (0–10 m depth), from ICES (1996)

Ship	Station	Latitude	Longitude	Year	Month	Day	Temp (°C)	Salinity (psu)	Chlorophyll <i>a</i> (mg/m <sup>3</sup> )
Tydeman	56	62.383	−4.683	86	6	15	9.17	35.21	8.6
Tydeman	57	62.150	−4.000	86	6	15	9.15	35.20	9.2
Tydeman	58	62.033	−3.650	86	6	15	8.70	35.18	9.2
Tydeman	70	62.040	−1.621	86	6	17	9.25	35.16	18.7
Tydeman	71	62.215	−2.125	86	6	17	9.25	35.19	24.3
Tydeman	72	62.356	−2.593	86	6	17	9.16	35.20	8.7
Tydeman	73	62.445	−2.837	86	6	17	9.21	35.20	9.2
Tydeman	74	62.601	−3.305	86	6	17	8.33	35.05	42.4
Tydeman	75	62.572	−4.557	86	6	17	9.38	35.21	8.6
Tydeman	76	62.682	−4.464	86	6	17	9.05	35.19	6.7
Tydeman	77	62.784	−4.378	86	6	17	8.06	34.99	22.2
Tydeman	78	62.967	−4.291	86	6	18	8.25	35.07	34.5
Tydeman	79	63.101	−2.038	86	6	18	9.02	35.17	14.4
Tydeman	80	62.824	−1.295	86	6	18	9.52	35.17	19.4
Tydeman	81	62.570	−0.666	86	6	18	9.58	35.17	18.3
Tydeman	82	62.334	−0.048	86	6	18	9.54	35.18	14.8
Tydeman	83	62.220	0.282	86	6	18	9.63	35.20	18.7
Tydeman	84	62.150	0.482	86	6	18	9.76	35.24	17.6
Tydeman	85	62.002	0.805	86	6	19	9.75	35.29	6.3
Tydeman	90	62.066	2.767	86	6	19	8.70	33.90	22.9
Tydeman	91	62.162	3.324	86	6	19	8.94	33.03	15.5
Tydeman	92	62.212	3.601	86	6	19	8.43	33.49	15.8
Tydeman	93	62.242	3.758	86	6	19	9.28	32.01	20.1
Tydeman	94	62.348	4.354	86	6	19	8.94	31.20	21.5
Tydeman	95	62.536	3.935	86	6	19	8.80	33.58	30.3
Tydeman	96	62.624	3.742	86	6	19	8.88	33.84	17.2
Tydeman	97	62.711	3.601	86	6	20	9.43	35.20	15.5
Tydeman	98	62.887	3.187	86	6	20	9.10	35.20	16.2
Tydeman	99	63.093	2.724	86	6	20	9.18	35.17	15.5
Tydeman	100	63.385	2.052	86	6	20	9.29	35.14	10.6
Tydeman	101	63.624	1.556	86	6	20	9.37	35.14	14.8
Tydeman	102	63.717	1.300	86	6	20	9.50	35.19	17.6
Tydeman	103	64.000	0.750	86	6	20	9.03	35.11	18.0
Tydeman	104	64.300	0.000	86	6	20	9.00	35.16	12.7
Tydeman	106	65.117	−1.733	86	6	21	8.56	35.04	13.7
Tydeman	107	65.294	−2.013	86	6	21	8.98	35.13	20.4
Tydeman	109	64.418	−5.249	86	6	22	7.82	34.91	14.1
Tydeman	110	63.967	−5.233	86	6	22	9.28	35.07	6.7
Tydeman	111	63.383	−5.167	86	6	22	9.30	35.01	11.6
Tydeman	112	63.050	−5.433	86	6	22	10.20	35.20	4.4
Tydeman	113	62.933	−5.600	86	6	22	9.91	35.18	4.0
Tydeman	114	62.867	−5.667	86	6	22	10.03	35.18	5.5
Tydeman	115	62.817	−5.733	86	6	23	10.11	35.17	7.6
Tydeman	116	62.779	−5.775	86	6	23	10.12	35.17	5.4
Tydeman	117	62.744	−5.803	86	6	23	9.99	35.14	11.6
Tydeman	118	62.689	−5.865	86	6	23	10.05	35.20	2.8
Tydeman	119	62.615	−5.964	86	6	23	9.95	35.21	5.3
Scotia	84	62.283	−5.967	73	7	4	8.43	35.16	4.0
Scotia	86	62.450	−5.617	73	7	5	9.18	35.21	1.4
Scotia	87	62.467	−6.233	73	7	5	8.50	35.15	4.2
Scotia	88	62.567	−6.167	73	7	5	8.61	35.18	1.4
Scotia	89	62.483	−6.450	73	7	6	8.59	35.14	2.8

Table 7 (continued)

Ship	Station	Latitude	Longitude	Year	Month	Day	Temp (°C)	Salinity (psu)	Chlorophyll <i>a</i> (mg/m <sup>3</sup> )
Scotia	90	62.483	−6.583	73	7	6	8.73	35.14	2.3
Scotia	91	62.533	−6.550	73	7	6	8.62	35.15	2.6
Scotia	92	62.667	−6.467	73	7	6	9.74	35.21	0.5
Scotia	93	62.533	−7.067	73	7	6	8.62	35.16	2.9
Scotia	94	62.517	−7.367	73	7	7	8.70	35.16	2.2
Scotia	95	62.417	−7.500	73	7	7	8.83	35.15	1.3
Scotia	96	62.383	−7.283	73	7	7	9.10	35.16	0.9
Scotia	97	62.300	−7.917	73	7	7	8.86	35.15	1.7
Scotia	98	62.317	−8.333	73	7	8	9.40	35.21	0.9

Ling, 1969; Petrushevskaya and Bjørklund, 1974; Goll and Bjørklund, 1985). They concluded that the low abundances were probably a result of low radiolarian production, combined with opal fragmentation, dilution by input of minerogenic components, and chemical dissolution.

The low radiolarian numbers in the bottom sediments of the Lofoten Basin are probably a result of this high terrigenous input. This is in agreement with Paetsch et al. (1992) who indicate a high accumulation rate of terrigenous matter in the Norwegian Sea (Lofoten Basin), which they conclude to originate from the Norwegian continent. The continental slope off Møre is steep, and large slumping scars have been reported by several authors, e.g. Bugge et al. (1984).

Mica is the most common mineral component in the area of the Norwegian Basin where radiolarian fossils are sparse. Eisma and van der Gaast (1983) distinguished two mineral provinces in the Norwegian Sea: a basaltic province on the Iceland–Faeroe Ridge, with high concentrations of smectite, plagioclase and augite, and an acidic province along the Scotland–Shetland shelf, with high concentrations of illite, swelling illite and quartz. They also demonstrated how the distributions of these two mineral provinces, especially that of smectite, and the concentrations of coccoliths in Late Quaternary sediments reflected the change of current patterns during the most recent glacial–interglacial cycles. We suggest that the low opal radiolarian abundance in the bottom sediments of this area is caused by the masking effect of the slumped material. The high amount of mica gives further support to the idea of active slumping or mass transportation in the area.

The number of species (Appendix B) at each station has been plotted, Fig. 16. It is evident that most of the Atlantic domain is represented by high species numbers (>28), while most of the Polar and Arctic domains are represented by lower species numbers (<24). The contour lines for 24 and 28 species roughly enveloped the position of the Arctic front, an important oceanographic feature in the study area, which is located in the middle of the gradient of species number (Fig. 16). The number of species could therefore give a rough estimate of the position of the predominant water masses and oceanographic features, such as fronts, in the Norwegian–Iceland Seas in the geological record.

Factor 1 is focused on the western radiolarian abundance maxima, but also includes sediments to

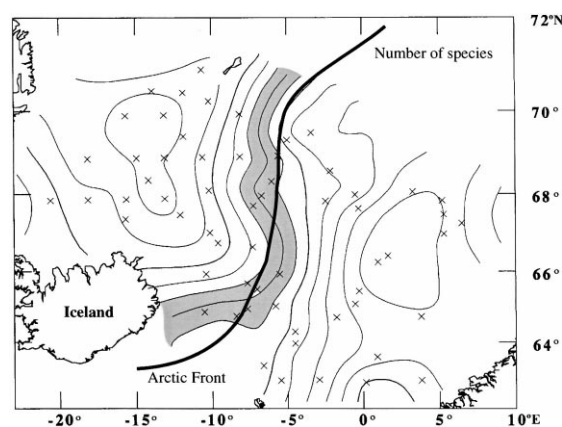


Fig. 16. Distribution of the number of radiolarian species in the GIN Seas. The area enveloped by the 24 and 28 species number isolines (shaded) and the position of the Arctic front are shown. Increment between isolines = 2; heavy line increment = 10.

the north with low radiolarian abundances (Figs. 4 and 11). Therefore Factor 1 is not a solution artifact.

Factor 2 is focused well to the east of the radiolarian abundance maxima. The highest factor loadings (Fig. 12) are within the 10 000–20 000 radiolarian abundance contours (Fig. 4). The 0.5 factor loading contour includes the two eastern radiolarian abundance maxima.

Factors 1 and 2 are essentially mutually exclusive. The 0.6 factor loading contours of the two factors almost coincide.

Factor 3 includes the northern radiolarian abundance maximum (Fig. 4), but extends to the south and has its highest value north of the southern radiolarian abundance maximum. Factor 3 is centered immediately to the east of the 0.6 factor loading contour for the two previous factors (Fig. 13), forming the boundary between Factors 1 and 2. Factor 3 has its highest values between the 0.5 and the 0.8 factor loading contours of Factor 2.

The northern radiolarian high abundance area, Fig. 4, could be interpreted as a single high production area. However, it is subdivided by the Arctic Front and therefore represents two different production areas.

Furthermore, the two Norwegian Sea abundance areas to the east of the Arctic Front could be interpreted as a single production area mirroring the AW. The separation into a southern and a northern abundance area, Fig. 4, could be a result of dissolution or sediment dilution, probably caused by slumping from the Vøring Plateau area to the east.

When plotting the selected varimax factor loading of 0.500 for Factor 1 and 0.700 for Factor 2, the isolines for these factor loadings coincide almost perfectly north of 66°N latitude in the Norwegian Sea, Fig. 17. This area also corresponds with the geographical position of Factor 3, interpreted as the area where mixing of warm Atlantic and cold Arctic water takes place, and also depicts the position of the Arctic Front.

In the southeast Factor 1 makes a large lobe extending towards The Faeroe Islands. In this area there is no match between the 0.500 Factor 1 isoline and the position of the Arctic Front. We interpret this discrepancy as a result of two signals, the Arctic Front being defined on a surface water temperature and salinity signal, while Factor 1 is signalling the

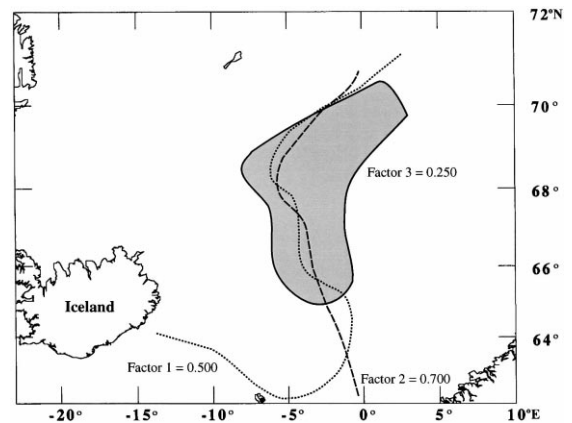


Fig. 17. Position of factor component isolines: Factor 1 (0.500, dotted line), Factor 2 (0.700, dashed line), and Factor 3 (0.250, full line). Factor component values higher than 0.500 for Factor 1 are found west of the dotted line, higher than 0.700 for Factor 2 east of the dashed line, and higher than 0.250 for Factor 3 within the shaded area.

subsurface radiolarian production zone, in this case *Amphimelissa setosa* which is the most predominant species in Factor 1.

### 5.3. Radiolarian preservation

Consideration of the preservation quality of the skeletons is essential for the discussion of radiolarian skeletal assemblages in the bottom sediments. Stadum and Ling (1969) reported on the exceptionally high abundance of phaeodarian skeletons in the surface sediments of the Norwegian and Iceland Seas. Bjørklund (1984) reported seven phaeodarian species from the region, and in the present study we have identified two more.

That the phaeodarians are relatively common in Norwegian Sea surface sediments suggests that the silica preservation is good, as phaeodarians are normally the first siliceous radiolarians to disappear from the sediment assemblage (Takahashi, 1981; Takahashi and Honjo, 1981). Since Phaeodaria are reported in higher abundances in cold water (Takahashi, 1987; Bernstein et al., 1990; Abelmann and Gowing, 1996) than in warm water regions, their high primary abundance might be the major point for preservation.

In core V27-46, on the Iceland Plateau, Kellogg (1975) recorded three distinct carbonate high peaks:

at 0–30 cm, corresponding to the Holocene; at ca. 300 cm, corresponding to the Eemian (isotopic stage 5e); and at ca. 1030 cm, extrapolated to an age of ca. 433 000 years (isotopic stage 11). Biogenic opal (diatoms, polycystine radiolarians and phaeodarians) is rich in the upper carbonate peak, while in the Eemian section biogenic opal is absent (Bjørklund, 1984). He also reported that phaeodarians were present at ca. 1030 cm to the bottom of the core, but that no diatoms or polycystine radiolarians were observed. This clearly shows that the accumulation and preservation of opal microfossils during three of the last interglacial periods have different opal signatures.

Data on the dissolved silica (as silicate) content in the bottom water from the Norwegian Sea, the Iceland Plateau, and the Cape Verde–Madeira Abyssal Plain were obtained from the GEOSECS database (GEOSECS, 1980), Table 8. The dissolved silica concentration in the GEOSECS data was between 9 and 15  $\mu\text{moles/kg}$  on the Iceland Plateau and 13–15  $\mu\text{moles/kg}$  in the Norwegian Basin, or about one fourth of the silica concentration in the North Atlantic bottom waters (46 to 48  $\mu\text{moles/kg}$  in the stations sampled in the Cape Verde–Madeira Abyssal Plain). The silica concentration in North Atlantic bottom waters is particularly high where the influence of Antarctic Bottom Water is felt. The presence of phaeodarian skeletons and the high abundances of opaline polycystine radiolarians in the surface

sediments of the GIN Seas must be due to some factor other than high silica concentration. This is supported by Sugiyama and Anderson (1997) who stated, for living rads in culture, that: “. . . changes in seawater silicate may not have a dramatic effect on longevity, skeletal size, or weight of some radiolarians. Thus other environmental variables, such as variations in temperature and salinity, may more likely impress a relatively more salient signal in the microfossil record”.

Distributions of phaeodarian skeletons and volcanic glass overlap in the GIN Seas, but do not correlate strongly (extreme examples include core V30-147, abundant in ash, but barren in phaeodarians, and core V28-42, abundant in phaeodarians, but barren in ash-shards). The presence of phaeodarian skeletons in surface sediments is always associated with good preservation of other opal microfossil groups, such as diatoms and polycystine radiolarians. We conclude that there is no direct correlation between the opal radiolarian preservation and the amount of volcanic glass, nor do the numerous volcanic ash shards have any significant influence on the dissolved silica values in the bottom waters of the Norwegian Sea and the Iceland Plateau.

## 6. Conclusions

(1) It was possible to recognize three species associations (factors) in the study area, and to plot their geographic position.

(2) The correlation coefficients obtained between seasonal sea surface temperature and Factors 1 ( $R^2 = 0.835$ ), and 2 ( $R^2 = 0.891$ ) show a very good fit, while for Factor 3 ( $R^2 = 0.497$ ) the correlation, although still significant at the 5% confidence level, was not as clear as for the first two factors. The factors correlated better with the summer than the winter sea surface temperatures.

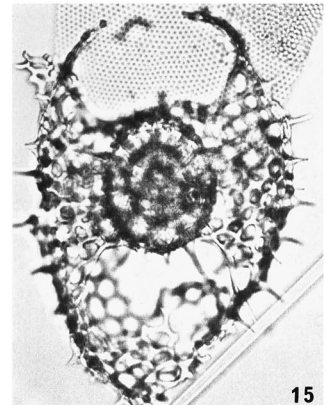
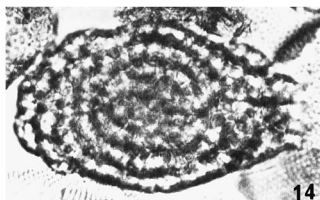
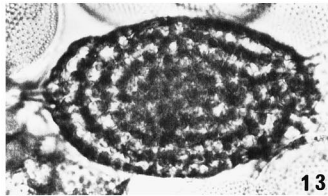
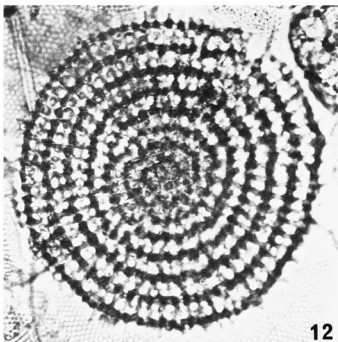
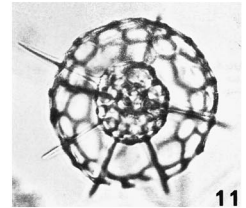
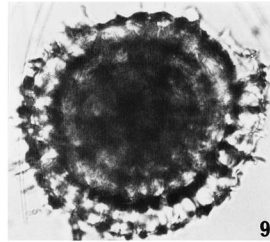
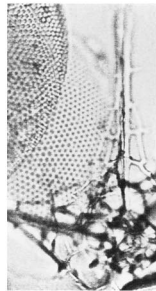
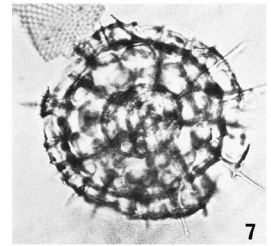
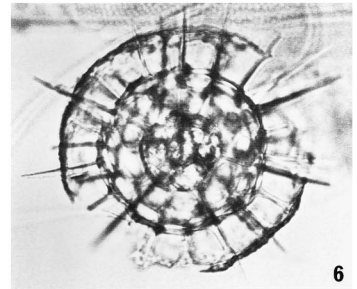
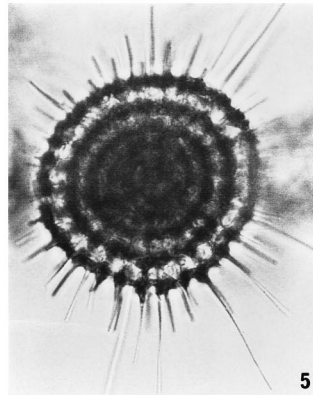
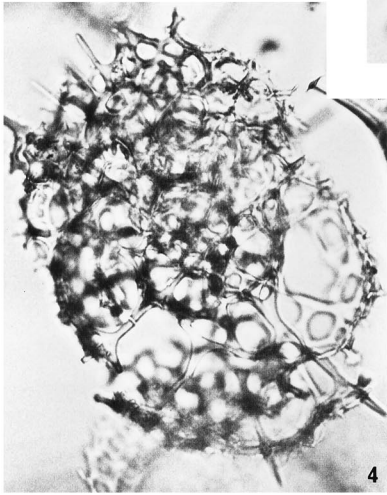
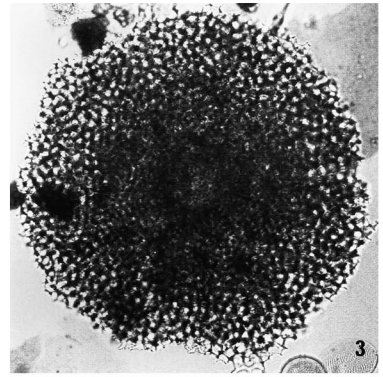
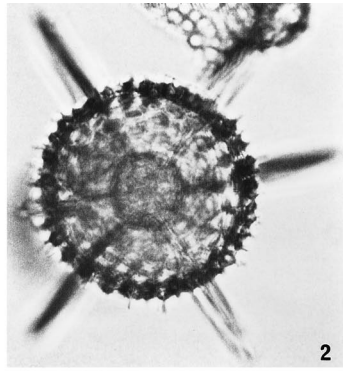
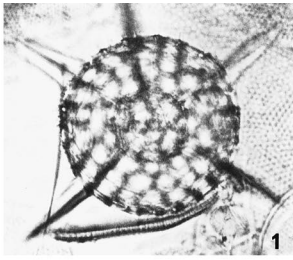
(3) Good correlation between temperature and factor scores is found for the winter temperature dataset at 50, 100 and 200 m water depth, Table 6. Our working hypothesis is that the eastward migration of the Arctic Front (and of the East Iceland Current, carrying the dominant species *Amphimelissa setosa*) is the reason for this good correlation.

(4) There was a trend of improving correlation coefficients with depth between factor scores and

Table 8  
GEOSECS (1980) sampling station identification numbers, their latitude and longitude, dissolved silica measurement and sampling water depth

GEOSECS Station ID	Latitude (°N)	Longitude (°W)	$\text{SiO}_3^{2-}$ ( $\mu\text{mole/kg}$ )	Water depth (m)
15	69.013	20.027	11.1	1526
16	72.042	8.442	10.2	2537
17	74.933	1.120	9.4	3682
18	70.000	0.008	13.3	3243
19	64.200	5.568	14.3	3458
22	61.655	14.292	11.9	1829
23	60.143	18.617	11.0	2516
114	21.175	21.775	48.8	4342
115	28.025	26.000	48.9	5303
116	29.933	30.400	46.2	4672

Latitude and longitude in decimal notation.





temperatures, with the best fit at 200 m for Factors 1 and 3 and at 100 m for Factor 2. This indirectly confirms that the optimal living depth for radiolarians is not at the surface, but deeper.

(5) The correlation between Factors 1–3 and phosphate, silicate, nitrate measurements from different depths of the GIN Seas was significant at the 5% confidence level, with very few exceptions.

This correlation decreases with depth and can be interpreted as caused by the fact that radiolarians are mainly feeding on primary producers, therefore there should be an indirect correlation with nutrients.

(6) The highest species richness for polycystine radiolarians (>28 species) was found in the warm Atlantic domain, the lowest (<24 species) was found in the colder arctic and polar domains.

An area approximating the position of the Arctic front had between 24 and 28 species, being located in the middle of the gradient of species number. This number could be used for a rough estimate of the position of the predominant water masses and oceanographic features, such as fronts, in the Norwegian–Iceland Seas in the geological record.

## Acknowledgements

The factor analysis package, originally designed for use with mainframe computers during the CLIMAP Project Members (1981) program, has

been modified for usage on IBM-PC platforms by T. Schrader. The Lamont-Doherty Earth Observatory of Columbia University (Palisades, NY, USA), the Department of Oceanography, University of Washington (Seattle, WA) and the Geological Institute, University of Bergen (Norway) are all acknowledged for providing the core-top material used in this study (cores recovered during cruises of the research vessels Vema, Edisto and Håkon Mosby, respectively). Support for the curatorial facilities of the Lamont-Doherty Earth Observatory Deep-Sea Sample Repository is provided by the National Science Foundation through Grant OCE94-02150 and the Office of Naval Research through Grant N00014-90-J-1060. Some of the temperature, salinity and all of the nutrient data used in this paper were provided by the ICES Oceanographic Data Centre (ocean@ices.dk). These data were provided to ICES from a variety of sources, in particular various North European marine institutes. Drs. Robert M. Goll, Stanley Kling, Dave Lazarus and an anonymous reviewer critically read and improved the manuscript. Their comments and discussions are gratefully acknowledged. Giuseppe Cortese would like to thank the following institutions for the economic support during the realization of the manuscript: the Paleontological Museum (University of Oslo), the Norwegian Research Council (KAS fellowship) and the Norwegian Academy of Sciences through the program 'Nansenfondet og de Dermed forbundne fond'.

## Appendix A

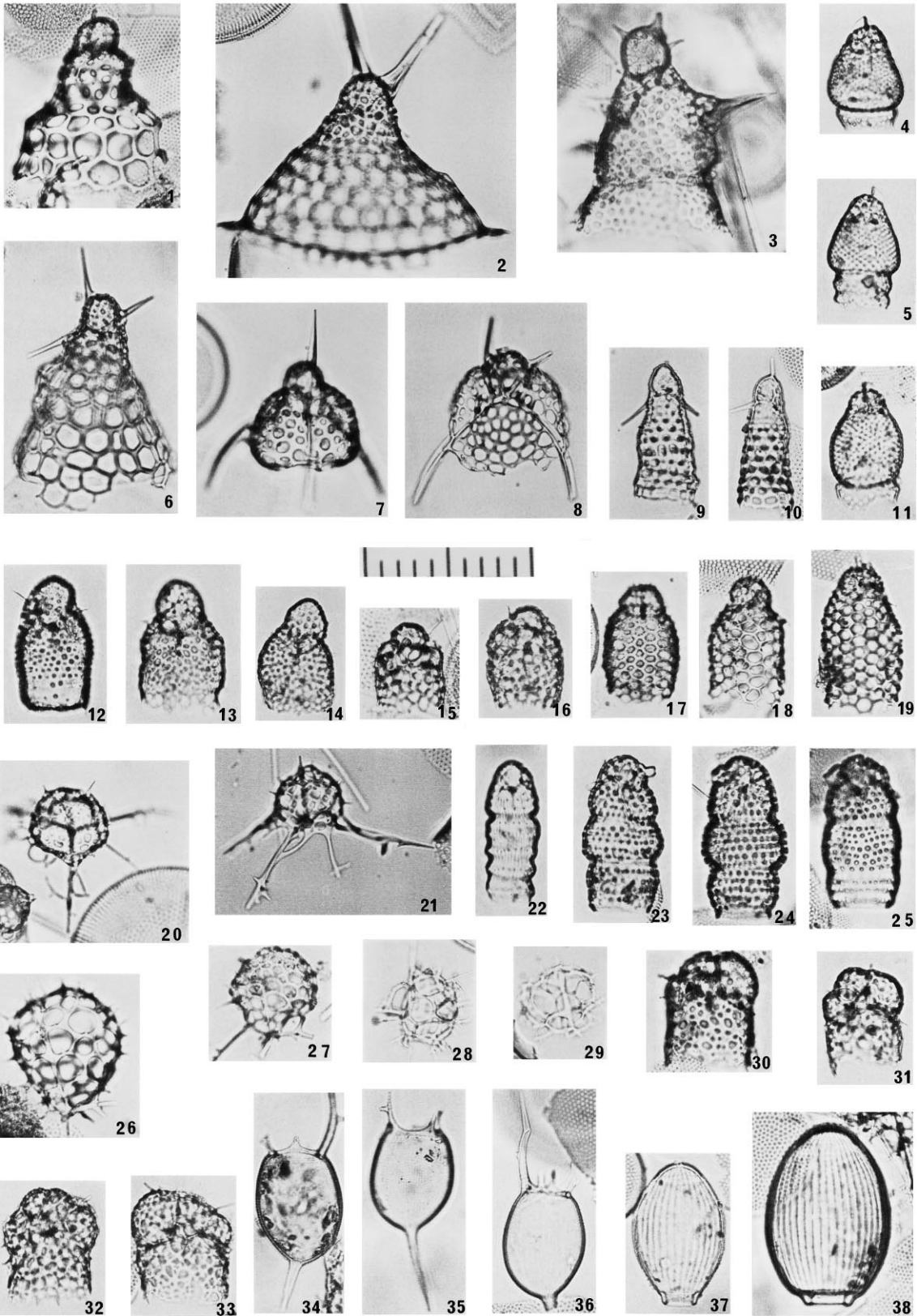
Taxa identified during this study, their author, and reference to photographs in the plates.

### Plate I

Plate 1, 9 and Plate 2, 28–29 are from the surface sample of core V29-219. All other specimens are from the surface sample of core V28-55. Scale bar is 100 µm for all photographs.

1. *Hexacantium pachydermum* Jørgensen, 1900
2. *Hexacantium pachydermum* Jørgensen, 1900
3. *Spongostrochus glacialis* Popofsky, 1908
4. *Streblacantha* sp. 1
5. *Larcospira minor* (Jørgensen, 1900)
6. *Actinomma boreale* Cleve, 1899
7. *Rhizoplegma boreale* (Cleve, 1899)
8. *Rhizoplegma boreale* (Cleve, 1899)
9. *Lithelius spiralis* Haeckel, 1860
10. *Actinomma boreale* Cleve, 1899
11. *Actinomma leptoderma leptoderma* (Jørgensen, 1900)
12. *Stylodictya validispina* Jørgensen, 1905
13. *Larcospira* sp. 1
14. *Larcospira* sp. 1
15. *Phorticium clevei* (Jørgensen, 1900)

Species	Author	Plate
<b>Spurnellaria</b>		
<i>Actinomma boreale</i>	Cleve, 1899	Plate I, 6, 10
<i>Actinomma leptoderma leptoderma</i>	(Jørgensen, 1900)	Plate I, 11
<i>Hexacantium pachydermum</i>	Jørgensen, 1900	Plate I, 1–2
<i>Larcospira</i> sp. 1	–	Plate I, 13–14
<i>Urcospira minor</i>	(Jørgensen, 1900)	Plate I, 5
<i>Lithelius spiralis</i>	Haeckel, 1860	Plate I, 9
<i>Phorticium clevei</i>	(Jørgensen, 1900)	Plate I, 15
<i>Rhizoplegma boreale</i>	(Cleve, 1899)	Plate I, 7–8
<i>Spongostrochus glacialis</i>	Popofsky, 1908	Plate I, 3
<i>Streblacantha</i> sp. 1	–	Plate I, 4
<i>Stylodictya validispina</i>	Jørgensen, 1905	Plate I, 12



**Nassellaria**

<i>Amphimelissa setosa</i>	(Cleve, 1899)	Plate II, 30–33
<i>Artobotrys boreale</i>	(Cleve, 1899)	Plate II, 4, 5, 11
<i>Artostrobos annulatus</i>	(Bailey, 1856)	Plate II, 9, 10
<i>Artostrobos joergenseni</i>	Petrushevskaya, 1971	Plate II, 17–19
<i>Corocalyptra craspedota</i>	(Jørgensen, 1900)	Plate II, 2
<i>Cycladophora davisiana</i>	(Ehrenberg, 1862)	Plate II, 1, 6
<i>Lipmanella xiphophorum</i>	(Jørgensen, 1900)	Plate II, 3
<i>Lithocampe platycephala</i>	(Ehrenberg, 1872)	Plate II, 23–25
<i>Lithomelissa hystrix</i>	Jørgensen, 1900	Plate II, 15, 16
<i>Lithomelissa setosa</i>	Jørgensen, 1900	Plate II, 12–14
<i>Lithomitra lineata</i>	(Ehrenberg, 1839)	Plate II, 22
<i>Peridium longispinum</i>	Jørgensen, 1900	Plate II, 26, 27
<i>Plectacantha oikiskos</i>	Jørgensen, 1900	Plate II, 28, 29

## Plate II

- Cycladophora davisiana* (Ehrenberg, 1862)
- Corocalyptra craspedota* (Jørgensen, 1900)
- Lipmanella xiphophorum* (Jørgensen, 1900)
- Artobotrys boreale* (Cleve, 1899)
- Artostrobos boreale* (Cleve, 1899)
- Cycladophora davisiana* (Ehrenberg, 1862)
- Pseudodictyophimus gracilipes* (Bailey, 1856)
- Pseudodictyophimus gracilipes* (Bailey, 1856)
- Artostrobos annulatus* (Bailey, 1856)
- Artostrobos annulatus* (Bailey, 1856)
- Artobotrys boreale* (Cleve, 1899)
- Lithomelissa setosa* Jørgensen, 1900
- Lithomelissa setosa* Jørgensen, 1900
- Lithomelissa setosa* Jørgensen, 1900
- Lithomelissa hystrix* Jørgensen, 1900
- Lithomelissa hystrix* Jørgensen, 1900
- Artostrobos joergenseni* Petrushevskaya, 1971
- Artostrobos joergenseni* Petrushevskaya, 1971
- Artostrobos joergenseni* Petrushevskaya, 1971
- Tholospyris gephyristes* Hülsemann, 1963
- Tholospyris gephyristes* Hülsemann, 1963
- Lithomitra lineata* (Ehrenberg, 1839)
- Lithocampe platycephala* (Ehrenberg, 1872)
- Lithocampe platycephala* (Ehrenberg, 1872)
- Lithocampe platycephala* (Ehrenberg, 1872)
- Peridium longispinum* Jørgensen, 1900
- Peridium longispinum* Jørgensen, 1900
- Plectacantha oikiskos* Jørgensen, 1900
- Plectacantha oikiskos* Jørgensen, 1900
- Amphimelissa setosa* (Cleve, 1899)
- Amphimelissa setosa* (Cleve, 1899)
- Amphimelissa setosa* (Cleve, 1899)
- Amphimelissa setosa* (Cleve, 1899)
- Euphysetta nathorstii* Cleve, 1899
- Euphysetta nathorstii* Cleve, 1899
- Euphysetta nathorstii* Cleve, 1899
- Euphysetta nathorstii* Cleve, 1899
- Lirella melo* (Cleve, 1899)
- Lirella melo* (Cleve, 1899)

<i>Pseudodictyophimus gracilipes</i>	(Bailey, 1856)	Plate II, 7, 8
<i>Tholospyris gephyristes</i>	Hülsemann, 1963	Plate II, 20, 21

**Phaeodaria**

<i>Euphysetta nathorstii</i>	Cleve, 1899	Plate II, 34–36
<i>Lirella melo</i>	(Cleve, 1899)	Plate II, 37, 38

**Spumellaria**

<i>Actinomma leptoderma longispina</i>	Cortese and Bjørklund (1998)
<i>Actinomma</i> sp. 1	–
<i>Actinomma trinacrium</i>	Haeckel, 1862
<i>Anomalocantha dentata</i>	(Mast, 1910)
<i>Cenosphaera favosa</i>	Haeckel, 1887
<i>Collosphaera murrayana</i>	(Haeckel, 1887)
<i>Euchitonina furcata</i>	Ehrenberg, 1872
<i>Hexacantium enthacantium</i>	Jørgensen, 1900
<i>Hexacantium hostile</i>	Cleve, 1900
<i>Hexalonche</i> sp. 1	–
<i>Spirema haliomma</i>	(Ehrenberg, 1861)
<i>Spongocore puella</i>	Haeckel, 1887
<i>Streblacantha circumtexta</i>	(Jørgensen, 1900)
<i>Stylatractus</i> sp. 1	–
<i>Styptosphaera spumacea</i>	Haeckel, 1887

**Nassellaria**

<i>Acanthocorys umbellifera</i>	(Haeckel, 1862)
<i>Acanthocyrtilis anthemis</i>	Haeckel, 1887
<i>Androcyclas gamphonycha</i>	(Jørgensen, 1900)
<i>Amphiplecta acrostoma</i>	Haeckel, 1887
<i>Botryostrobos</i> sp. 1	–
<i>Botryostrobos tumidulus</i>	(Bailey, 1856)
<i>Campylacantha cladophora</i>	Jørgensen, 1905
<i>Carpocanarium papillosum</i>	(Ehrenberg, 1872)
<i>Carpocanistrum</i> sp. 1	–
<i>Ceratocyrtilis galleus</i>	(Cleve, 1899)
<i>Ceratocyrtilis hystrix</i>	(Jørgensen, 1905)
<i>Ceratospyrilis hyperborea</i>	Jørgensen, 1905
<i>Cladoscenium limbatum</i>	Jørgensen, 1905
<i>Cladoscenium tricolpium</i>	(Haeckel, 1881)
<i>Cornutella profunda</i>	Ehrenberg, 1854
<i>Eucyrtidium</i> sp. 1	–
<i>Eucyrtidium</i> sp. 2	–
<i>Euscenium corynephorum</i>	Jørgensen, 1900
<i>Lamprocyclas maritilis</i>	Haeckel, 1887
<i>Litharachnium tentorium</i>	Haeckel, 1862
<i>Lithomelissa</i> sp. aff.	Bjørklund, 1976
<i>L. stigi</i>	
<i>Lithomelissa thoracites</i>	Haeckel, 1862
<i>Nephrospyris knutheieri</i>	Goll and Bjørklund, 1985
<i>Phormacantha hystrix</i>	(Jørgensen, 1900)
<i>Plagiacantha arachnoides</i>	Claparède, 1855
<i>Plectophora triacantha</i>	Popofsky, 1908
<i>Protocystis</i> sp. 1	–
<i>Pterocorys cranoides</i>	(Haeckel, 1862)
<i>Stichocorys seriata</i>	Jørgensen, 1905
<i>Theocorythium trachelium</i>	(Ehrenberg, 1872)
<i>Trissocyclis</i> sp. 1	–

**Phaeodaria**

<i>Porospatis halostoma</i>	(Cleve, 1899)
-----------------------------	---------------















## References

- Abelmann, A., Gowing, M.M., 1996. Horizontal and vertical distribution pattern of living radiolarians along a transect from the Southern Ocean to the South Atlantic subtropical region. *Deep-Sea Res.* 43 (3), 361–382.
- Bailey, J.W., 1856. Notice of microscopic forms found in the soundings of the Sea of Kamtschatka: with a plate. *Am. J. Sci. Arts, Second Ser.* 64, 1–6.
- Bé, A.W.H., Hutson, W.H., 1977. Ecology of planktonic foraminifera and biogeographic patterns of life and fossil assemblages in the Indian Ocean. *Micropaleontology* 23 (4), 369–414.
- Bernstein, R.E., Betzer, P.R., Takahashi, K., 1990. Radiolarians from the western North Pacific Ocean: a latitudinal study of their distributions and fluxes. *Deep-Sea Res.* 37 (11), 1677–1696.
- Bjørklund, K.R., 1973. The seasonal occurrence and depth zonation of radiolarians in Korsfjorden, western Norway. *Sarsia* 56, 13–42.
- Bjørklund, K.R., 1976. Radiolaria from the Norwegian Sea, Leg 38 of the Deep Sea Drilling Project. In: Talwani, M., Udintsev, G. et al. (Eds.), Initial Reports of the Deep Sea Drilling Project 38, 1101–1168. U.S. Government Printing Office, Washington DC.
- Bjørklund, K.R., 1984. Euphysetta (Phaeodaria, Radiolaria) in the Norwegian–Greenland Sea sediments (distribution in space and time). *Euro-rad IV, Fourth International meeting of radiolarists*, Leningrad, USSR, Oct. 15–19 1984, pp. 239–244.
- Bjørklund, K.R., Swanberg, N.R., 1987. The distribution of two morphotypes of the radiolarian *Amphimelissa setosa* Cleve (Nassellarida): A result of environmental variability? *Sarsia* 72, 245–254.
- Bjørklund, K.R., Ciesielski, P.F., 1994. Ecology, morphology, stratigraphy, and the paleoceanographic significance of *Cycladophora davisiana davisiana*. Part I: Ecology and morphology. *Mar. Micropaleontol.* 24, 71–88.
- Bugge, T., Knarud, R., Mørk, A., 1984. Bedrock geology on the mid-Norwegian continental shelf. In: *Norw. Pet. Soc., A.M. Spencer et al. (Eds.), Petroleum Geology of the North European Margin*. Graham and Trotman, London, pp. 271–283.
- Claparède, E., 1855. Über die Lebenserscheinungen und insbesondere Bewegungsercheinungen der Acanthometren. *Monatsber. Kgl. Preuss. Akad. Wiss. Berlin, Jahrg.* 1855, 674–676.
- Cleve, P.T., 1899. Plankton collected by the Swedish expedition to Spitzbergen in 1898. *Köngl. Svenska Vetenskaps-Akad. Handl.* 32, 1–51.
- Cleve, P.T., 1900. Notes on some Atlantic plankton-organisms. *Köngl. Svenska Vetenskaps-Akad. Handl.* 34 (1), 1–22.
- Cortese, G., Bjørklund, K.R., 1998. The taxonomy of boreal Atlantic Ocean Actinommida (Radiolaria). *Micropaleontology*, in press.
- Dietrich, G., 1969. Atlas of the Hydrography of the North Atlantic Ocean Based on the Polar Survey of the International Geophysical Year, Winter and Summer 1958. Compiled by G. Dietrich. Conseil International pour l'exploration de la mer, Service hydrographique. Charlottenlund Slot, Denmark.
- Dolven, J.K., 1998. Late Pleistocene to Late Holocene biostratigraphy and paleotemperatures in the SE Norwegian Sea, based on Polycystine radiolarians. Master Degree Thesis, Faculty of Mathematics and Natural Sciences, University of Oslo.
- Ehrenberg, C.G., 1839. Über die Bildung der Kreidelfelsen und des Kreidemergels durch unsichtbare Organismen. *Abh. Kgl. Akad. Wiss. Berlin, Jahrg.* 1838, 59–147.
- Ehrenberg, C.G., 1854. *Mikrogeologie*. Voss, Leipzig, 374 pp.
- Ehrenberg, C.G., 1861. Über den Tiefgrund des stillen Ozeans zwischen Californien und den Sandwich-Inseln aus bis 15.000 Fuss Tiefe nach Lieut. Brookes. *Monatsber. Kgl. Preuss. Akad. Wiss. Berlin*, 819–833.
- Ehrenberg, C.G., 1862. Über die Tiefgrund-Verhältnisse des Ozeans am Eingange der Davisstrasse und bei Island. *Monatsber. Kgl. Preuss. Akad. Wiss. Berlin, Jahrg.* 1861, 275–315.
- Ehrenberg, C.G., 1872. Mikrogeologischen Studien als Zusammenfassung seiner Beobachtungen des kleinstens Lebens der Meeres-Tiefgrunde aller Zonen und dessen geologischen Einfluss. *Monatsber. Kgl. Preuss. Akad. Wiss. Berlin, Jahrg.* 1872, 265–322.
- Eisma, D., van der Gaast, S.J., 1983. Terrigenous Late Quaternary sediment components north and south of the Scotland–Greenland Ridge and in the Norwegian Sea. In: Bott, M.H.P., Saxov, S., Talwani, M., Thiede, J. (Eds.), *Structure and development of the Greenland–Scotland Ridge: new methods and concepts*. NATO Conf. Ser. IV. Marine Sci. 8, 607–636.
- Eldholm, O., Skogseid, J., Sundvor, E., Myhre, A.M., 1990. The Norwegian–Greenland Sea. In: Grantz, A., Johnson, L., Sweeney, J.F. (Eds.), *The Geology of North America*. vol. L. The Arctic Ocean Region. Geological Society of America, Boulder, CO, pp. 351–364.
- Gauch, H.G. Jr., 1982. *Multivariate analysis in community ecology*. Cambridge: Cambridge University Press.
- Geochemical Ocean Sections Program (GEOSECS): collected papers, 1976–1979, 1980. *Earth Planet. Sci. Lett.*, 49(2), 259–564.
- Goll, R.M., Bjørklund, K.R., 1974. Radiolaria in surface sediments of the South Atlantic. *Micropaleontology* 20, 38–75.
- Goll, R.M., Bjørklund, K.R., 1985. *Nephrospyris knutheieri* sp. n., an extant trisocyclid radiolarian (Polycystinea: Nassellarida) from the Norwegian–Greenland Sea. *Sarsia* 70, 103–118.
- Haeckel, E., 1860. Über neue, lebende Radiolarien des Mittelmeeres. *Monatsber. Kgl. Preuss. Akad. Wiss. Berlin, Jahrg.* 1860, 794–817.
- Haeckel, E., 1862. Die Radiolarien (Rhizopoda radiata). Eine Monographie. Berlin, 572 pp.
- Haeckel, E., 1881. Entwurf eines Radiolarien-Systems auf Grund von Studien der Challenger. Radiolarien. *Jenaische Z. Naturwiss.* 15, 418–472.
- Haeckel, E., 1887. Report on the Radiolaria collected by H.M.S. Challenger during the years 1873–1876. *Report Sci. Results, Voyage Challenger, Zoology* 18 (2 parts), 1–1803.
- Hopkins, T.S., 1988. The GIN Sea: Review of physical oceanography and literature from 1972. *SACLANT Undersea Research*

- Center, La Spezia, Italy. SACLANTCEN Report SR-124, 190 pp.
- Hutson, W.H., 1980. The Agulhas Current during the Late Pleistocene. Analysis of modern faunal analogs. *Science* 207, 64–66.
- Hülsemann, K., 1963. Radiolaria in plankton from the Arctic Drifting Station T-3, including the description of three new species. *Arctic Inst. N. Am. Tech. Pap.* 13, 1–52.
- ICES, 1996. International Council for the Exploration of the Sea, Oceanographic Data Centre, Copenhagen, Denmark.
- Imbrie, J., Kipp, N.G., 1971. A new micropaleontological method for quantitative paleoclimatology: application to a late Pleistocene Caribbean core. In: Turekian, K.K. (Ed.), *The late Cenozoic glacial ages*. Yale University Press, New Haven, pp. 71–147.
- Jansen, E., Bjørklund, K.R., 1985. Surface ocean circulation in the Norwegian Sea 15,000, B.P. to present. *Boreas* 14, 243–257.
- Johannessen, T., Jansen, E., Flatøy, A., Ravelo, A.C., 1994. The relationship between surface water masses, oceanographic fronts and paleoclimatic proxies in surface sediments of the Greenland, Iceland, Norwegian Seas. In: Zahn, R., Pedersen, T.F., Kaminski, M.A., Labeyrie, L. (Eds.), *Carbon cycling in the Glacial ocean: constraints on the ocean's role in global change. Quantitative approaches in paleoceanography*. NATO ASI Series, 117. Springer-Verlag, Berlin, Heidelberg.
- Jørgensen, E., 1900. Protistenplankton aus dem Nordmeere in den Jahren 1897–1900. *Bergens Museums Aarbog* 1899 6, 45–98.
- Jørgensen, E., 1905. The protist plankton and the diatoms in bottom samples. In: O. Nordgaard (Ed.), *Hydrographical and biological investigations in Norwegian fiords*. Bergens Museum Skrifter 1(7), 59–151.
- Kellogg, T.B., 1975. Late Quaternary climatic changes in the Norwegian and Greenland Seas. In: Weller, G., Bowling, S.A. (Eds.), *Climate of the Arctic*. University of Alaska Press, Fairbanks, pp. 3–36.
- Kellogg, T.B., 1976. Late Quaternary climatic changes: evidence from deep-sea cores of Norwegian and Greenland Seas. In: Cline, R.M., Hays, J.D. (Eds.), *CLIMAP-Investigation of Late Quaternary paleoceanography and paleoclimatology*. *Geol. Soc. Am. Mem.* 145, 77–110.
- Kellogg, T.B., 1984. Late glacial–Holocene high-frequency climatic changes in deep-sea cores from the Denmark Strait. In: Mörner, N.A., Karlön, W. (Eds.), *Climatic Changes on a Yearly to Millennial Basis*. Reidel, Hingham, pp. 123–133.
- Klován, J.E., Imbrie, J., 1971. An algorithm and FORTRAN-IV program for large-scale Q-mode factor analysis and calculation of factor scores. *J. Indian Soc. Soil Sci.* 3 (1), 61–77.
- Koç-Karpuz, N., Schrader, H., 1990. Surface sediment diatom distribution and Holocene paleotemperature variations in the Greenland, Iceland and Norwegian seas. *Paleoceanography* 5, 557–580.
- Koç, N., Jansen, E., Hafliðason, H., 1993. Paleoceanographic reconstructions of surface ocean conditions in the Greenland, Iceland and Norwegian seas through the last 14 ka based on diatoms. *Quat. Sci. Rev.* 12, 115–140.
- Koç, N., Jansen, E., Hald, M., Labeyrie, L., 1996. Late glacial–Holocene sea surface temperatures and gradients between the North Atlantic and the Norwegian Sea: implications for the Nordic heat pump. In: Andrews, J.T., Austin, W.E.N., Bergsten, H., Jennings, A.E. (Eds.), *Late Quaternary Palaeoceanography of the North Atlantic Margins*. *Geol. Soc. Spec. Publ.* 111, 177–185.
- Kruglikova, S.B., 1977. Atlas of micro-organisms in bottom sediments of the oceans. Diatoms, Radiolarians, Silicoflagellates, Cocoliths. Jouse, A.P. (Ed.). Nauka, Moscow, pp. 13–17 and plates 86–145.
- Le, J., Shackleton, N.J., 1994. Reconstructing paleoenvironment by transfer function: model evaluation with simulated data. *Mar. Micropaleontol.* 24, 187–199.
- Levitus, S., 1982. *Climatological atlas of the world ocean*. U.S. Government Printing Office, Washington, D.C., NOAA Prof. Pap. 13, 173 pp.
- Mast, H., 1910. Die Astrosphaeriden. *Wiss. Ergebn. Deutschen Tiefsee-Expedition Valdivia* 19 (4), 123–190.
- Molina-Cruz, A., Bernal-Ramirez, R.G., 1996. Distribution of Radiolaria in surface sediments and its relation to the oceanography of the Iceland and Greenland Seas. *Sarsia* 81, 315–328.
- Morley, J.J., 1983. Identification of density stratified waters in the Late Pleistocene North Atlantic: A faunal derivation. *Quat. Res.* 20, 374–386.
- Morley, J.J., Hays, J.D., 1979. *Cycladophora davisiana*: A stratigraphic tool for Pleistocene North Atlantic and interhemispheric correlation. *Earth Planet. Sci. Lett.* 44, 383–389.
- Niiler, P.P., Piacsek, S., Neuberg, L., Warn-Varnas, A., 1992. Sea surface temperature variability of the Iceland–Faeroe Front. *J. Geophys. Res.* 97 (C11), 17777–17785.
- Paetsch, H., Botz, R., Scholten, J.C., Stoffers, P., 1992. Accumulation rates of surface sediments in the Norwegian–Greenland Sea. *Mar. Geol.* 104, 19–30.
- Petrushevskaya, M.G., 1967. Radiolarians of orders Spumellaria and Nassellaria of the Antarctic region. In: Andriyashev, A.P., Ushakov, P.V. (Eds.), *Biological Reports of the Soviet Antarctic Expedition (1955–1958)* 3, 2–186 (in Russian, English edition 1968).
- Petrushevskaya, M.G., 1971. Radiolyarii Nassellaria v planktone Mirovogo Okeana. *Issledov. Fauna Morei SSSR* 9 (17), 5–249.
- Petrushevskaya, M.G., Bjørklund, K.R., 1974. Radiolarians in Holocene sediments of the Norwegian–Greenland Seas. *Sarsia* 57, 33–46.
- Pflaumann, U., Duprat, J., Pujol, C., Labeyrie, L.D., 1996. SIM-MAX: A modern analog technique to deduce Atlantic sea surface temperatures from planktonic foraminifera in deep-sea sediments. *Paleoceanography* 11 (1), 15–35.
- Popofsky, A., 1908. Die Radiolarien des Antarktis. *Deutsche Sudpolar Exped.*, 1901–03 10, 184–305.
- Samtleben, C., Schäfer, P., Andruleit, H., Baumann, A., Baumann, K.-H., Kohly, A., Matthiessen, J., Schröder-Ritzrau, A., 1995. Plankton in the Norwegian–Greenland Sea: from living communities to sediment assemblages — an actualistic approach. *Geol. Rundsch.* 84 (1), 108–136.
- Sarnthein, M., Altenbach, A.V., 1995. Late Quaternary changes in surface water and deep water masses of the Nordic Seas

- and north-eastern Atlantic: a review. *Geol. Rundsch.* 84 (1), 89–107.
- Schröder, O., 1909. Die nordischen Spumellarien. II. Unterlegion Sphaerellarien. *Nordisches Plankton* 7 (17), 1–66.
- Schröder, O., 1914. Die nordischen Nassellarien. *Nordisches Plankton* 7 (17), 67–140.
- Schäfer, P., Thiede, J., Gerlach, S., Graf, G., Zeitschel, B., 1995. Global environmental change: the northern North Atlantic. *Geol. Rundsch.* 84 (1), 3–10.
- Seidov, D., Sarnthein, M., Stattegger, K., Prien, R., Weinelt, M., submitted. North Atlantic ocean circulation during the last glacial maximum and subsequent meltwater event: a numerical model. *J. Geophys. Res.* 101, 16305–16332.
- Stadum, C.J., Ling, H.Y., 1969. Tripylean Radiolaria in deep-sea sediments of the Norwegian Sea. *Micropaleontology* 15 (4), 481–489.
- Sugiyama, K., Anderson, O.R., 1997. Experimental and observational studies of radiolarian physiological ecology, 6. Effects of silicate-supplemented seawater on the longevity and weight gain of spongioid radiolarians *Spongaster tetras* and *Dictyocoryne truncatum*. *Mar. Micropaleontol.* 29, 159–172.
- Swanberg, N.R., Bjørklund, K.R., 1986. The radiolarian fauna of western Norwegian fjords: patterns of abundance in the plankton. *Mar. Micropaleontol.* 11, 231–241.
- Swanberg, N.R., Eide, L.K., 1992. The radiolarian fauna at the ice edge in the Greenland Sea during summer, 1988. *J. Mar. Res.* 50, 297–320.
- Swift, J.H., Aagaard, K., 1981. Seasonal transitions and water mass formation in the Iceland and Greenland seas. *Deep-Sea Res.* 28 (10), 1107–1129.
- Takahashi, K., 1981. Vertical flux, ecology and dissolution of Radiolaria in tropical oceans: implications for the silica cycle. Ph.D. thesis, Woods Hole Oceanographic Institution, 461 pp.
- Takahashi, K., 1987. Radiolarian flux and seasonality: climatic and El Niño response in the Subarctic Pacific, 1982–1984. *Global Biogeochem. Cycles* 1 (3), 213–231.
- Takahashi, K., Honjo, S., 1981. Sinking speed, residence time and dissolution of Radiolaria. In: *The Geological Society of America, 94th annual meeting. Abstracts with Programs, Geological Society of America* 13(7), 564.
- Tolderlund, D.S., Bé, A.W.H., 1971. Seasonal distribution of planktonic foraminifera in the western North Atlantic. *Micropaleontology* 17 (3), 297–329.
- U.S. Navy Hydrographic Office (USNHO), 1958. *Oceanographic atlas of the polar seas, Pt. II, Arctic*. Washington, DC.
- U.S. Naval Oceanographic Office (USNOO), 1967. *Oceanographic atlas of the North Atlantic Ocean, Sec. 2, Physical properties*. Washington, DC.
- Wiborg, K.F., 1955. Zooplankton in relation to hydrography in the Norwegian Sea. *Fiskeridirektoratets Skrifter, Serie Havundersøkelser (Report on Norwegian Fishery and Marine Investigations)* XI(4), 1–66.